JCTC Journal of Chemical Theory and Computation

Global Hybrid Functionals: A Look at the Engine under the Hood

Gábor I. Csonka,*[,†,‡] John P. Perdew,[‡] and Adrienn Ruzsinszky[‡]

Department of Inorganic and Analytical Chemistry, Budapest University of Technology and Economics, H-1521 Budapest, Hungary and Department of Physics and Quantum Theory Group, Tulane University, New Orleans, Louisiana 70118, United States

Received August 26, 2010

Abstract: Global hybrids, which add a typically modest fraction of the exact exchange energy to a complement of semilocal exchange−correlation energy, are among the most widely used density functionals in chemistry and condensed matter physics. Here we briefly review the formal and practical advantages and disadvantages of global hybrids. We point out that empiricism seems unavoidable in the construction of global hybrids, as it is not for most other kinds of density functional. Then we use one to three parameters to hybridize many semilocal functionals (including recently developed nonempirical generalized gradient approximations or GGA's and meta-GGA's). We study the performance of these global hybrids for many properties of sp-bonded molecules composed from the lighter atoms of the periodic table: atomization energies, barrier heights, reaction energies, enthalpies of formation, total energies, ionization potentials, electron affinities, proton affinities, and equilibrium bond lengths. We find several new global hybrids that perform better in these tests than standard ones, and we correct some errors in literature assessments. We also discuss the representativity of small fitting sets and the adequacy of various Gaussian basis sets.

1. Introduction to Semilocal and Global Hybrid Functionals

For the description of electronic states in atoms, molecules, and solids, correlated wave function methods can be accurate but very expensive. Kohn and Sham[1] showed that, given the exact density functional for the exchange−correlation energy, the ground-state energy and density of interacting electrons in a multiplicative external potential could be found exactly and efficiently from a single Slater determinant of self-consistent orbitals that see a multiplicative effective potential. The exchange−correlation energy arises from the tendency of electrons to avoid one another due to fermion antisymmetry and Coulomb repulsion. Without it, chemical binding would be weak or absent.[2]

The exact exchange−correlation energy can be expressed as a coupling constant integration or adiabatic connection formula:[3−45]

$$E_{xc} = (1/2)\int d^3r \int d^3r'\, n(\vec{r}) n_{xc}(\vec{r},\vec{r}')/|\vec{r}'-\vec{r}| \quad (1)$$

Here $n_{xc}(\vec{r},\vec{r}') = n_x(\vec{r},\vec{r}') + n_c(\vec{r},\vec{r}')$ is the density at position $\vec{r}'$ of the exchange−correlation hole around an electron at $\vec{r}$. Note that

$$n_{xc}(\vec{r},\vec{r}') = \int_0^1 d\lambda [n_x(\vec{r},\vec{r}') + n_{c,\lambda}(\vec{r},\vec{r}')] \quad (2)$$

is averaged over the strength λ of the Coulomb repulsion $\lambda/|\vec{r}' - \vec{r}|$ at fixed electron density $n(\vec{r})$. The holes satisfy important sign and sum rules:[3−5]

$$n_x(\vec{r},\vec{r}') \le 0, \quad \int d^3r' n_x(\vec{r},\vec{r}') = -1, \quad \int d^3r' n_c(\vec{r},\vec{r}') = 0 \quad (3)$$

* Address correspondence to csonkagi@gmail.com.
† Budapest University of Technology and Economics.
‡ Tulane University.

10.1021/ct100488v © 2010 American Chemical Society
Published on Web 11/18/2010

The first approximation for the spin density functional for exchange and correlation, the local spin density approximation[1,6,7] (LSDA), was constructed to be exact for a uniform electron gas and subsequently shown[3−5] to satisfy the hole constraints of eq 3. Later semilocal functionals[8−15] were constructed nonempirically to satisfy these and many other physical or exact constraints. Although recent nonempirical functionals are not constructed from hole models, constraint-satisfying hole models[16−18] have been reverse engineered from them. All nonempirical semilocal functionals, including LSDA, are by construction exact in the uniform density limit. Some semilocal functionals (e.g., refs 19 and 20) have also been constructed empirically, by fitting to chemical data.

A semilocal (sl) spin density functional:

$$E_{\mathrm{xc}}^{\mathrm{sl}}[n_\uparrow, n_\downarrow] = \int \mathrm{d}^3 r n(\vec{r}) \varepsilon_{\mathrm{xc}}^{\mathrm{sl}}(n_\uparrow(\vec{r}), n_\downarrow(\vec{r}), \nabla n_\uparrow(\vec{r}), \nabla n_\downarrow(\vec{r}), \tau_\uparrow(\vec{r}), \tau_\downarrow(\vec{r})) \quad (4)$$

can be evaluated as a computationally efficient single integral, using ingredients available at position $\vec{r}$, such as the local spin densities $n_\sigma(\vec{r})$ with $\sigma = \uparrow$ or $\downarrow$ (as in LSDA) or additionally their gradients $\nabla n_\sigma(\vec{r})$ as in a generalized gradient approximation (GGA)[8−12,14,19,20] or further the spin-resolved positive orbital kinetic energy densities $\tau_\sigma(\vec{r})$ (as in a meta-GGA).[12,15,21] Fully nonlocal approximations,[22] which require a double integral as in eq 1, can be considerably more costly. For this reason, an efficient method[23] was developed to deal with the full nonlocality of an early van der Waals density functional.[24] Semilocal approximations can be expected to work only when the exact exchange−correlation hole density is well-localized around its electron,[25] as it is in atoms and in many molecules and solids near equilibrium, and even when (at both the interacting and noninteracting levels, the latter possibly with the help of symmetry breaking)[26] electrons are not shared between separated subsystems in the dissociation limit.[27] However, stretched bonds that arise in transition states of chemical reactions or in the dissociation limits of some radical or heteronuclear molecules, etc., require full nonlocality.[25,28−30] Long-range van der Waals interactions also require full nonlocality.

In a typical atom, exchange and correlation can be separately described by good semilocal functionals. In the valence region of a typical molecule near equilibrium, both the exact exchange energy and the exact correlation energy are fully nonlocal, but their full nonlocalities tend to cancel. Thus semilocal approximations for the exchange−correlation energy can work even there. This error cancellation arises because the exact n_{xc} tends to be deeper and more short-ranged in $|\vec{r}' - \vec{r}|$ (and thus more semilocal) than either the exact $n_{\mathrm{x}}(\vec{r},\vec{r}')$ or the exact $n_{\mathrm{c}}(\vec{r},\vec{r}')$ alone. While the dynamic correlation energy of the molecule is approximated by $E_{\mathrm{c}}^{\mathrm{sl}}$, its static or left-right[31] fully nonlocal correlation energy can be estimated from the negative quantity $(E_{\mathrm{x}}^{\mathrm{sl}} - E_{\mathrm{x}}^{\mathrm{exact}}) - \sum(\mathrm{atoms})(E_{\mathrm{x}}^{\mathrm{sl}} - E_{\mathrm{x}}^{\mathrm{exact}})$, where the last sum is over the constituent free atoms.

The global hybrid (gh) idea, due to Becke,[32,33] introduces some full nonlocality into the calculation but only at the level of $E_{\mathrm{x}}^{\mathrm{exact}}$, which can be evaluated semianalytically from the Kohn−Sham orbitals in some computer codes. In its simplest (one parameter) version:[34]

$$E_{\mathrm{xc}}^{\mathrm{gh}} = aE_{\mathrm{x}}^{\mathrm{exact}} + (1 - a)E_{\mathrm{x}}^{\mathrm{sl}} + E_{\mathrm{c}}^{\mathrm{sl}} \quad (5)$$

where the exact-exchange mixing parameter a takes an empirical value in the range $0 \le a \le 1$. For a in this range, both a and $1 - a$ are positive, so all the hole constraints of eq 3 are preserved, including the sign constraint on n_{x}. Because the hybrid functional statistically improves the atomization energies over its semilocal parent, a better estimate of the static correlation energy in the molecule is thus $(1 - a)\{(E_{\mathrm{x}}^{\mathrm{sl}} - E_{\mathrm{x}}^{\mathrm{exact}}) - \sum(\mathrm{atoms})(E_{\mathrm{x}}^{\mathrm{sl}} - E_{\mathrm{x}}^{\mathrm{exact}})\}$, which is more nearly independent of the choice of $E_{\mathrm{x}}^{\mathrm{sl}}$ when a is fitted to the atomization energies for that choice. Because eq 5 is linear in $E_{\mathrm{x}}^{\mathrm{exact}}$, it is properly size extensive: It makes the energy of a system of well-separated subsystems equal to the sum of the energies of the subsystems. Nonlinear mixing should only (and cautiously) be done at deeper levels of the exact-exchange ingredient, such as the exact-exchange energy density $n(\vec{r})\varepsilon_{\mathrm{x}}^{\mathrm{exact}}(\vec{r})$ (as in the local hybrids[25] discussed around eq 6) or even the exact-exchange hole density $n_{\mathrm{x}}^{\mathrm{exact}}(\vec{r},\vec{r}')$ (as in range-separated hybrids, e.g., ref 35). Note that the range-separated or screened exchange hybrid of Heyd, Scuseria, and Ernzerhof (HSE)[36] is designed to imitate the performance of the standard Perdew−Burke−Ernzerhof (PBE) global hybrid PBE0, while eliminating some of the practical problems of exact exchange in metals.

Perhaps the most convincing argument for eq 5 is the least sophisticated one: Semilocal exchange−correlation typically overestimates atomization energies and underestimates energy barriers to chemical reactions, while exact exchange without correlation makes errors of the opposite sign, so that mixing of the two will yield better atomization energies and barriers than either alone.

Becke[32] also justified eq 5 on the basis of the adiabatic connection in eqs 1 and 2: The errors of semilocal exchange and correlation are expected to cancel substantially at $\lambda = 1$ but cannot cancel at $\lambda = 0$ where only the exchange hole survives (since $n_{\mathrm{x}} \sim \lambda^0$, while $n_{c,\lambda} \sim \lambda^1$), so some exact exchange should be mixed with semilocal exchange−correlation. This argument has been quantified[34] to predict a mixing parameter $a = 0.25$, which is the basis for the standard PBE hybrid PBE0.[37,38] This prediction for a uses a model for the λ dependence of $\Delta E_{\mathrm{c},\lambda}$ and must be understood for what it is. First, it applies only to atomization energies, not to other properties. Second, it relies on the qualitative empirical observation that fourth-order perturbation theory in the electron−electron interaction is fairly accurate for atomization energies. Third, even for atomization energies (or for formation enthalpies based upon calculated atomization energies), it is only a rough estimate, reliable within perhaps a factor of 2. As we will see below, values of a fitted to formation enthalpies vary from from 0.60 for PBEsol[14] GGA to 0.32 for the PBE[11] GGA to 0.1 for the Tao−Perdew−Staroverov−Scuseria (TPSS)[13] and revised TPSS (revTPSS)[15] meta-GGA's. Improving the underlying semilocal functional reduces the value of a needed to fit the atomization energies or formation enthalpies and so worsens the barrier heights. The converse is that semilocal functionals

with highly overestimated atomization energies, like the PBE variant for solids (PBEsol),[14] can hybridize to produce excellent barrier heights, as we will also show. Some global hybrids[39,40] thus employ highly fitted semilocal parts intended not to be accurate by themselves but to work well with a fraction of exact exchange. Starting from a standalone semilocal functional, some fraction of exact exchange can be expected to improve most calculated properties, but there is no reason to expect that a single fraction will be optimal for most or all.

Global hybrids with $a < 1$ typically satisfy most of the exact constraints satisfied by the underlying semilocal functional (and all of those for TPSS and revTPSS) but cannot satisfy any additional exact constraints and thus are unavoidably empirical. To satisfy additional constraints and to make optimum use of sophisticated nonempirical meta-GGA's, one can go to the local hybrid[25,41,42] (lh) level in which the mixing fraction $a(\vec{r})$ varies with position:

$$E_{xc}^{lh} = \int d^3r\, n(\vec{r})[a(\vec{r})\varepsilon_x^{exact}(\vec{r}) + \{1 - a(\vec{r})\}\varepsilon_x^{sl}(\vec{r})] + E_c^{sl} \quad (6)$$

where $\varepsilon_x(\vec{r})$ is the exchange energy per electron at $\vec{r}$. But local hybrids seem to require even more empirical parameters than global hybrids do, because the additional exact constraints are only limits: Parameters are needed to control how these limits are approached.[25] Local hybrids also have a potential problem which global ones do not: the nonuniqueness of energy densities like $n(\vec{r})\varepsilon_x(\vec{r})$.[43,44]

Global hybrids often achieve useful accuracy, even in cases where their success is unexplained. They improve atomization energies and related formation enthalpies of molecules as well as energy barriers for reasons we have already discussed. But they also improve equilibrium bond lengths, and they can slightly improve or worsen total energies, ionization energies, electron affinities, and proton affinities,[45] as we shall see below. In solid-state physics, they can often improve the description of strongly correlated solids.[46] Improvements to fundamental band gaps[47] and point defect energies[48] have also been reported. It should be remembered, however, that the improved orbital-energy gaps arise from the use of a fraction of the nonmultiplicative Hartree−Fock exchange potential. Using instead an optimized effective Kohn−Sham multiplicative potential for the fraction of exact exchange would reduce the orbital-energy gaps back to the semilocal range, without much affecting ground-state energies and energy differences.[49,50] Thus explanations of the solid-state successes of global hybrid functionals, based upon their improved orbital-energy gaps, are unconvincing or at least incomplete. There are also documented cases where standard global hybrids are consistently less accurate or as inaccurate as semilocal functionals, including properties of transition-metal compounds[51] and the adsorption energies of CO on transition-metal surfaces.[52]

While the exact total energy of a separated open system varies linearly as a function of average electron number between adjacent integers,[53] the energy predicted by a semilocal density functional approximation is concave upward, and the exact-exchange or Hartree−Fock energy is concave downward.[54] As a result, semilocal functionals can fail[53] for separated open systems of fluctuating electron number, such as the fragments of stretched molecular AB[28,55] or A_2^+.[29] Global hybrid functionals with sufficient exact exchange can clearly fix these problems,[55] in part. For example, we have computed the many-electron self-interaction error[29] $\Delta = E(He_2^+, R = 200\ Å) - E(He) - E(He^+)$, for which the exact value is 0 kcal/mol. We find that Δ is determined mainly by the value of a, and not by the choice of semilocal functional, and that Δ is almost linear in a. With the very different semilocal functionals BPW91, PBE,[11] or PBEsol,[14] we find $\Delta = -96$ kcal/mol for $a = 0$ and $\Delta = -31$ kcal/mol for $a = 0.60$. We observed a similar tendency for dissociating Li_2^+ and F_2^+.

In the next section, we will discuss three-parameter global hybrids as originally proposed by Becke,[32] which not only fit a fraction of exact exchange but also scale the gradient or inhomogeneity corrections to LSDA in the underlying semilocal functional. Our plausibility arguments for this are that the optimal inhomogeneity corrections are less well-known (and indeed less well-defined for a given set of arguments in eq 4) than is the uniform-density limit and that the optimal inhomogeneity corrections change when some exact exchange is included. Then we will construct one- or three-parameter global hybrids for many semilocal functionals, including the recently developed PBEsol[14] GGA and revTPSS[15] meta-GGA that have not been hybridized before, and assess them for a wide range of molecular properties.

2. B3PW91 and B3LYP Functionals

In 1993 Becke suggested the B3PW91 functional in the following form:[32]

$$E_{xc}^{B3PW91} = a \cdot E_x^{exact} + (1 - a) \cdot E_x^{LSDA} + b \cdot \Delta E_x^{B88} + E_c^{LSDA} + c \cdot \Delta E_c^{PW91} \quad (7)$$

where b and c are multiplying factors that modify the exchange and correlation gradient corrections, respectively. Note that choice $b = 1 - a$ and $c = 1$ leads to eq 5 when the semilocal functional is BPW91 (B88 GGA exchange[19] plus PW91 GGA correlation).[10] Because the b and c parameters provide more freedom than the single-parameter hybrid of eq 5, the three-parameter form of eq 7 can give somewhat better results if all three parameters are fitted to experimental data. (We denote our new one parameter hybrids with a subscript a, as in BPW91h$_a$, and our new three parameter hybrids with a subscript abc, as in BPW91h$_{abc}$). Later the B3LYP empirical hybrid functional[56] was constructed with exactly the same $a = 0.2$, $b = 0.72$, and $c = 0.81$ parameters proposed by Becke but with PW91 correlation swapped out. Instead the linear combination $(1 - c) \cdot E_c^{SVWN3} + c \cdot E_c^{LYP}$ was used for the correlation energy in eq 7, where E_c^{SVWN3} is the LSDA correlation energy in the random phase approximation (which does not yield the correct PW92[7] or SVWN5[57] homogeneous electron gas limit). The LYP functional is self-correlation error free, but it does not give the correct uniform gas limit and so produces serious errors for metallic solids.[58] However, despite these construction problems, the B3LYP functional delivered good

results for small molecules, and it was preferred in many areas of chemistry over the B3PW91 and other functionals. The evidence for this is strong. Each of refs 20 and 32 has been cited about 30 000 times, according to the Web of Science. Recent results show several serious failures of the B3LYP functional that may arise from its design problems.[59−64] B3PW91 gives consistently better results for large organic molecules.[45,60] This better performance of B3PW91 can be attributed to its correct behavior for the homogeneous electron gas. (A similar attribution was made for B3PW91 versus B3LYP atomization energies of metals).[63] Note that part of the self-interaction error of BPW91 is removed in B3PW91 and B3LYP.

3. Test Sets

We shall use the following test sets:

In their early works Adamo and Barone use zero-point energy (ZPE) corrected atomization energies, $\sum D_0$, of the small G2-32 test set to measure the performance of the one-parameter hybrids (cf. eq 5).[38,65] The G2-32 test set was derived from the G2/97 test set[66] by selecting the first 32 compounds that contain first-row elements (Z < 10).

The AE6 test set of Lynch and Truhlar[67] provides a quick and supposedly representative evaluation for the ZPE-subtracted atomization energy, $\sum D_e$, of diverse molecular systems. The set includes six molecules: SiH_4, S_2, SiO, C_3H_4, $C_2H_2O_2$, and C_4H_8.

The Kinetics9 database[68,69] contains three forward barrier heights, three reverse barrier heights, and three energies of reaction for the three reactions in the BH6[67] database. We use the optimized QCISD/MG3 geometries and the recent spin−orbit corrected reference energies for AE6 and BH6.[70]

The G3/99 test set[71] includes 223 standard enthalpies of formation (without deleting the COF_2 molecule, contrary to the recommendation in ref 71), 88 ionization potentials, 58 electron affinities, and 8 proton affinities for compounds that contain first- and second-row elements (Z < 18). For the development of the first hybrid functionals, a smaller G2/97 test set was used (148 standard enthalpies of formation). The G3-3 test set includes larger organic molecules and several problematic inorganic compounds. The G3-3 and the G2/97 test sets together form the G3/99 test set.

The IP86 test set for gas-phase ionization potentials was defined in ref 45. As the pure $a = 0$ functionals have convergence problems for H_2S^+ and N_2^+, these were left out from the 88 species of the original G3/99 test set.

The EA58 test set for gas-phase electron affinities and the PA8 test set for gas phase proton affinities were taken from the G3/99 test set.[71]

The T-96R contains equilibrium internuclear distances (r_e) of the 86 neutral diatomic molecules and 10 diatomic molecular cations.[45]

In this paper we shall show how one-parameter global hybrids can be constructed from the BLYP, BPW91, PBE, PBEsol, TPSS, and revTPSS functionals. The PBEsol and revTPSS functionals were programmed by us. As we show later, the selection of the PBEsol functional is particularly interesting as it overbinds the most among the functionals in this study. Thus it requires the largest exact-exchange fraction for optimal performance on atomization energy test sets. The results obtained by the new functionals will be compared to the results obtained by the original three-parameter B3PW91 and B3LYP functionals. We will discuss:

- The dependence of the results on the test sets and the representativity of the G2-32 and AE6 test sets compared to the G3/99 test set.
- The role of the basis sets.
- Is the original B3PW91 parametrization optimal for the G3/99 test set?
- How do parameter values influence the performance of the functionals?
- Is it possible to find better hybrid parameters for eqs 5 and 7 than the currently used values?

4. Thermochemical Properties

4.1. Results for the G2-32 Test Set. First we tried to reproduce the earlier[38,65] ZPE-corrected atomization energies, $\sum D_0$, for the hybrids B1LYP, B1PW91, and PBE0 constructed from the BLYP, BPW91, and PBE functionals for the G2-32 test set with $a = 0.25$. We use the Gaussian 03 program for all calculations,[72] the B3LYP/6-31G(2df, p) optimized geometries, the ultra-fine grid, and the 6-311++G(3df, 3pd) basis set, as in most of the original publications. The amount of 25% exact exchange was set via Iop(3/76 = 0750002500) of the GAUSSIAN 03 program. While we were able to reproduce PBE0 results,[38] our B1LYP and B1PW91 results deviate considerably from the earlier results[65] (cf. Supporting Information). According to our results the PBE0, B1LYP, and B1PW91 mean absolute errors (MAE) are 2.8, 4.8, and 5.0 kcal/mol, respectively, compared to the published 2.6, 3.1, and 5.4 kcal/mol.[38,65] Thus the good PBE0 results were reproduced, but the performance of B1LYP is not significantly better than that of B1PW91, in disagreement with the results of Adamo et al.[65] The differences between the published B1LYP and our results are the following (cf. Supporting Information): (1) The calculated $\sum D_0$ energies do not agree for BeH (ours vs Adamo et al.: 54.4 vs 48.5 kcal/mol), ethane (656.0 vs 654.1 kcal/mol), and hydrazine (402.1 vs 401.2 kcal/mol). For 22 compounds our results agree precisely, and for the other 7 compounds the difference is less than 0.6 kcal/mol. (2) Using the calculated $\sum D_0$ energies by Adamo et al., we obtain MAE = 4.8 kcal/mol, in agreement with our current results. Consequently the published value for the MAE of B1LYP (3.1 kcal/mol)[65] should be corrected. (See the detailed energies in the Supporting Information). Below we show that the BLYP functional is not suitable for the construction of a one parameter hybrid functional. The B1LYP functional yields worse thermochemistry than the BLYP functional for more adequate AE6 and G3/99 test sets. The origin of the 'success' of the B1LYP functional for the G2-32 test set is the inappropriate choice of the test set.

4.2. Results for the AE6, BH6, and K9 Test Sets. Next we used small but so-called representative test sets. Analysis of mean error (ME) and MAE of the thermochemical results obtained for AE6, BH6, and Kinetics9 shows the following

Table 1. Summary of Deviations (ME and MAE) from Experiment of the Atomization Energies in the AE6 set and the Reaction Energy Barriers in the BH6 set As Well As the RMSE for the Kinetics9 (K9) Test Set Calculated with the 6-311+G(3df, 3pd) Basis Set[a]

				AE6		BH6		K9
functional	*a*	*b*	*c*	ME	MAE	ME	MAE	RMSE
BLYP	0.00	1.00	1.00	−1.7	6.6	−8.1	8.1	7.1
BPW91	0.00	1.00	1.00	2.4	6.9	−7.7	7.7	6.9
PW86PBE	0.00	1.00	1.00	2.1	7.8	−8.1	8.1	7.4
PBE	0.00	1.00	1.00	12.3	15.3	−9.6	9.6	8.8
PBEsol	0.00	1.00	1.00	35.8	35.8	−13.0	13.0	12.0
TPSS	0.00	1.00	1.00	3.9	5.6	−8.6	8.6	7.4
revTPSS	0.00	1.00	1.00	3.1	5.9	−7.6	7.6	7.6
M05-2X	0.56	n.a.	n.a.	0.2	2.6	−0.5	**1.4**	**1.4**
M06-2X	0.54	n.a.	n.a.	−0.2	**1.2**	−0.7	**1.2**	**1.1**
B3LYP	0.20	0.72	0.81	−2.2	2.6	−5.1	5.1	4.5
B3PW91	0.20	0.72	0.81	−0.3	4.0	−4.7	**4.7**	**4.0**
BPW91h$_a$	0.10	0.90	1.00	−1.6	5.4	−5.9	5.9	5.2
BPW91h$_{abc}$	**0.15**	**0.75**	**0.35**	−0.5	**2.1**	−4.2	**4.2**	**4.0**
BPW91h$_{abc}$	0.15	0.79	0.75	−0.6	3.1	−5.0	**5.0**	**4.4**
BPW91h$_{abc}$	0.15	0.80	0.85	−0.6	3.7	−5.2	5.2	4.6
BPW91h$_{abc}$	0.15	0.81	0.95	−0.6	4.3	−5.4	5.4	4.8
BPW91h$_a$	0.15	0.85	1.00	−3.5	5.2	−5.1	5.1	4.5
PW86PBEh$_a$	0.15	0.85	1.00	−3.7	5.5	−5.4	5.4	4.9
BPW91h$_{abc}$	**0.20**	**0.70**	**0.57**	−0.6	**2.1**	−5.0	**5.0**	**4.4**
BPW91h$_{abc}$	0.20	0.72	0.77	−0.6	3.4	−4.6	**4.6**	**3.9**
BPW91h$_a$	0.20	0.80	1.00	−5.4	6.2	−4.2	**4.2**	**3.7**
BPW91h$_{abc}$	**0.21**	**0.70**	**0.57**	−1.8	**2.1**	−4.3	**4.3**	**3.7**
PBE0	0.25	0.75	1.00	0.3	6.2	−4.9	**4.9**	4.5
PBEh$_a$	**0.32**	**0.68**	**1.00**	−2.8	5.3	−3.7	**3.7**	**3.5**
PBEsolh$_a$	0.50	0.50	1.00	3.2	10.0	−2.6	**2.6**	**2.6**
PBEsolh$_a$	**0.60**	**0.40**	**1.00**	−2.9	11.1	−0.9	**1.4**	**1.8**
TPSSh	0.10	0.90	1.00	0.6	6.1	−7.0	7.0	6.3
revTPSSh$_a$	0.10	0.90	1.00	0.1	7.8	−6.2	6.2	6.7

[a] The weight of exact exchange (*a*) and the *b* and *c* parameters are also shown for the hybrid functionals (cf. eq 7). Note that one-parameter hybrids have $a > 0$, $b = 1 - a$, and $c = 1$. In our notation, h$_a$ and h$_{abc}$ denote global hybrids with new or refitted empirical parameters *a* and *a*, *b*, and *c*. Note also that Becke's original B3PW91 has $a = 0.20$, $b = 0.72$, and $c = 0.81$. All values are in kcal/mol. Error = theory − experiment. The results that are better than the B3LYP results are shown bold. The mean experimental atomization energy for AE6 is 517.8 kcal/mol, and the mean barrier height for BH6 is 11.7 kcal/mol.

(cf. Table 1): The ZPE-subtracted atomization energy, $\sum D_e$, results in Table 1 show that most of the GGA functionals yield positive ME for the AE6 test set (error = theory − experiment) and thus partly conserve the overbinding tendency of the LDA. PBEsol, which uses the exact second-order gradient coefficient for exchange valid for the slowly varying limit over a wide range of *s*, shows the largest overbinding, while PBE uses a coefficient about twice as big and shows a considerably reduced overbinding, about one-third of that for PBEsol. The BPW91, PW86PBE, TPSS, and revTPSS functionals give much better results, small but positive MEs (2−4 kcal/mol) and relatively small MAEs (6−8 kcal/mol). The TPSS and revTPSS functionals give the best results. The BLYP functional differs qualitatively from these functionals, as it underbinds slightly (ME = −1.7 kcal/mol).

Increasing the weight of the exact exchange according to eq 5 decreases the ME values (increases the underbinding). This leads to improvements of the MAE of the overbinding functionals for the AE6 test set (cf. BPW91h$_a$ and PBEh$_a$ in Figure 1). However, as the BLYP functional underbinds for the AE6 test set, no improvement is possible via exact exchange mixing alone (eq 5). The good B3LYP results for the AE6 test set mainly come from the reduced gradient contribution to the exchange and from mixing the LDA and LYP correlation functionals (cf. eq 7, *b* and *c* parameters and the results in the Table 1). Note that the BLYP functional overbinds for the G2-32 test set (ME = 4.3 kcal/mol, cf. Table S1, Supporting Information) and can be improved by the exact-exchange mixing according to eq 5. In order to resolve this contradiction between AE6 and G2-32 test set, we shall check the validity of these results on the large G3/99 test set (vide infra).

The BPW91, PW86PBE, PBE, and PBEsol overbinding for the AE6 test set is readily decreased by the simple inclusion of exact exchange (eq 5). We observed for BPW91h$_a$, PBEh$_a$, and PBEsolh$_a$ hybrids that the ME shows a quasilinear dependence on the value of the parameter *a*. Close to the optimal values of *a*, the slopes are −38 (BPW91h) and −45 kcal/mol (PBEh). Figure 1 shows how the larger positive ME is compensated by a larger amount of exact exchange for the BPW91 and PBE functionals. The optimal values for *a* are 0.15, 0.15, 0.32, and 0.5 for BPW91h$_a$, PW86PBEh$_a$, PBEh$_a$, PBEsolh$_a$, respectively (cf. Table 1). Notice that meta-GGAs behave differently. Inclusion of 10% of exact exchange worsens the MAEs for the AE6 test set despite some improvements for the MEs.

Applying $a = 0.2$ for the BPW91h$_{abc}$ hybrid as proposed by Becke gives too strong underbinding (cf. eq 5 and Table 1). However, this is compensated by the reduced exchange and correlation gradient contributions via *b* and *c* parameters in B3PW91 (cf. eq 7). The *b* and *c* parameters compensate each other's effect on the ME. A similar compensation effect was observed earlier for H_2 bond distance, total energy, and electron density.[73] We observed that, at fixed *a*, a 0.01 increase of the value of *b* is compensated by a 0.1 increase of the value of *c*. For the BPW91h hybrid functional with $a = 0.15$, we can obtain ME = −0.6 kcal/mol with several different combinations *b* and *c*. Table 1 shows that the same ME can be obtained with $b = 0.81$ and $c = 0.95$, $b = 0.80$ and $c = 0.85$, $b = 0.79$ and $c = 0.75$, or even $b = 0.75$ and $c = 0.35$. This latter combination provides also the smallest (2.1 kcal/mol) MAE, and this can be reproduced with $a = 0.20$, $b = 0.70$, and $c = 0.57$ values in eq 7. These BPW91h$_{abc}$ hybrids are considerably better than the B3LYP or B3PW91 functionals for the AE6 test set (cf. MAE = 2.6 and 4.0 kcal/mol, respectively, in Table 1). Note the excellent performances of the M05-[74] and M06-2X[75] functionals for these test sets (c.f. Table 1). The AE6 and BH6 species were included in the extensive (more than 400 species) fitting sets of these hybrid meta-GGA functionals. The M06-2X functional performs the best and it applies more than 30 fitted parameters. The M05- and M06-2X calculations were performed with the Gaussian 09 program.[76]

Table 1 shows that, among the semilocal functionals applied to the BH6 and K9 test sets, the revTPSS functional gives the best (but poor) results. The BPW91, BLYP, and PW86PBE results are only slightly worse. The PBE and PBEsol functionals give the worst results. The hybrids give

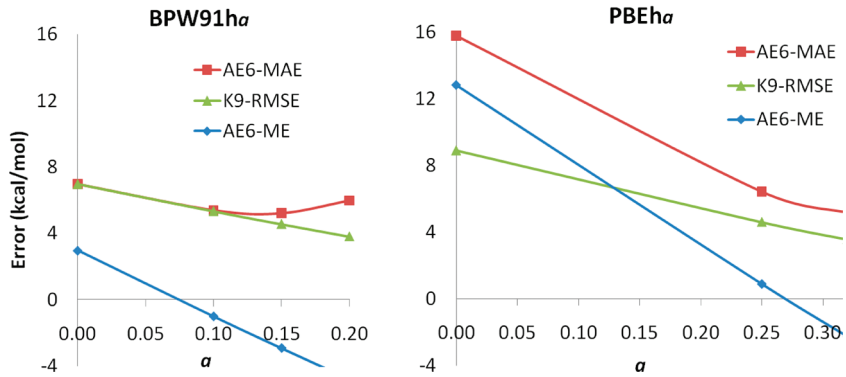

Figure 1. Quasilinear dependence of the ME for the AE6 test set as a function of the weight of exact exchange (*a*) for the BPW91 and PBE hybrids (cf. eq 5). The MAE for the AE6 test set and the RMSE for Kinetics9 (K9) test set are also shown.

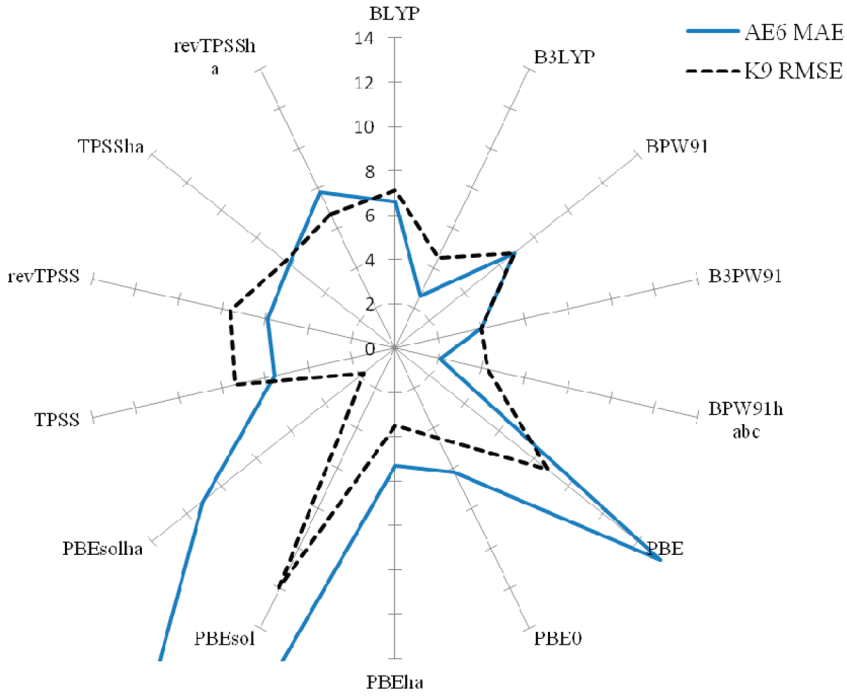

Figure 2. Radar or polar chart summary of the MAE's (kcal/mol) for the AE6 test set and the RMSEs (kcal/mol) for the Kinetics9 (K9) test set for several density functionals discussed in this paper. The connecting lines are simply for guiding the eye. Smaller value means better performance.

improved results for the energy barriers and for kinetics too. The larger weight of the exact exchange considerably decreases the root-mean-square errors (RMSE) for the K9 test sets, and $a = 0.6$ in eq 5 leads to the excellent performance of the PBEsol hybrid (RMSE = 1.8 vs 12.0 kcal/mol for PBEsol). Here again the M06-2X functional shows the best performance ($a = 0.54$, RMSE = 1.1 kcal/mol).

The statistical results for several nonempirical or at most three-parameter functionals are visualized in Figure 2. The radar chart of the MAEs (kcal/mol) for the AE6 test set and the RMSEs (kcal/mol) for the Kinetics9 (K9) test set shows the improvements due to the hybrid functional. Notice that B3PW91 improves the AE6 and K9 results about the same extent but B3LYP does not. BPW91h$_{abc}$ improves only the AE6 results compared to B3PW91. The new PBEh$_a$ ($a = 0.32$) results are uniformly better than those of the PBE0 ($a = 0.25$). Notice that the PBEsolh$_a$ functional performs poorly for the atomization energies (MAE = 11.1 kcal/mol). However, after removing the errors arising from the inconsistencies in the energies of the free atoms and molecules, as suggested in ref 60, we obtain MAE = 2.6 kcal/mol.

Figure 3 shows how the errors of individual PBEsol hybrid atomization energies for the molecules of the AE6 test set depend on the weight of the exact exchange. Increasing the weight of the exact exchange changes the atomization energies in the direction of underbinding for five molecules (see negative slopes in Figure 3), and the effect is the strongest for $C_2H_2O_2$. For SiH_4 the opposite effect can be observed: a very slight overbinding effect occurs. (See the positive slope in Figure 3.) The figure shows that the optimal value of a depends on the composition of the test set. Consequently it is advisible to use larger test sets for parameter optimizations (vide infra).

4.3. Results for the G3/99 Test Set. The results for the enthalpies of formation $\Delta_f H^0_{298}$ of the large G3/99 test set (223 enthalpies of formation) will be discussed here. In this work we apply the procedure of the G3X theory, which uses

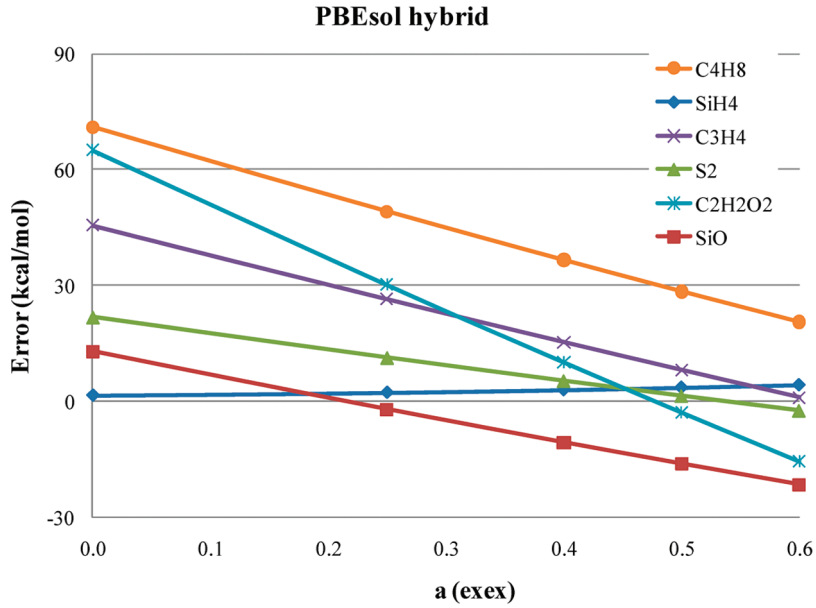

Figure 3. Quasilinear dependence of the errors of the atomization energies of the components of the AE6 test set as functions of the weight of exact exchange (*a*) for the PBEsol hybrid (cf. eq 5).

the equilibrium B3LYP/6-31G(2df, p) geometries in combination with the B3LYP/6-31G(2df, p) zero-point vibration energies and thermal corrections obtained with a frequency scale factor of 0.9854.[77] Note that the $\Delta_f H^0_{298}$ values are calculated from the negatives of the $\sum D_e$ values, atomic enthalpies, and thermal corrections; see eq 1 of ref 60. Thus a more negative ME of the calculated $\Delta_f H^0_{298}$ values means a change in the overbinding direction. The results in Table 2 show that BLYP underbinds (ME = 3.81 kcal/mol) in the same way as for the AE6 test set. Thus the overbinding experienced for the G2-32 test set is seemingly accidental, due to the nonrepresentativity of the latter test set. The other GGAs overbind the same way as for the AE6 test set (cf. ME = −5.6 kcal/mol for BPW91 or ME = −21.69 kcal/mol for PBE in Table 2). Here we include the combination of the PW86 exchange and the PBE correlation functional, since this functional is free of almost all the attractive dispersion forces for noble gas dimers, and thus it is particularly suitable for an additive dispersion correction.[78] We also include TPSS and revTPSS functionals that perform particularly well for thermochemistry even without the inclusion of the exact exchange. We shall present here the first hybrid constructed from revTPSS, the revTPSSh$_a$.[45]

Inspection of Table 2 shows that many of the new hybrid functionals perform considerably better than B3LYP or B3PW91 (cf. Table 2). The best performer is the BPW91h$_{abc}$ with $a = 0.20$, $b = 0.70$, and $c = 0.57$ (MAE = 3.1 kcal/mol). This result is better than the best results published in ref 45 for VSXC (MAE = 3.5 kcal/mol), but M06-2X remains the best performer with MAE = 2.6 kcal/mol (cf. Table 2). The BPW91h$_{abc}$ with $a = 0.21$, $b = 0.70$, and $c = 0.57$ (MAE = 3.3 kcal/mol) and with $a = 0.15$, $b = 0.75$, and $c = 0.35$ (MAE = 4.3 kcal/mol) performs worse. The next best performers are TPSSh and revTPSSh$_a$ with $a = 0.10$ (eq 5) (MAE = 3.9 and 4.3 kcal/mol, respectively). Table 2 also shows that the new PBEh$_a$ with $a = 0.32$ (eq 5) performs better than B3LYP (MAE = 4.7 vs 4.9 kcal/mol) or PBE0[37,38] with $a = 0.25$ in eq 5 (MAE = 6.7 kcal/mol). The revTPSS functional performs slightly better than TPSS (MAE = 5.1 vs 5.8 kcal/mol).

Comparison of the results obtained for the G3/99 and AE6 test sets shows that AE6 is suitable for rough parameter optimization; however, optimization on it does not yield precisely the optimal parameters for the G3/99 test set. For example we observed a considerable difference for the PBEsol hybrid. Optimization for the AE6 test gives $a = 0.5$ (cf. ref 79 and Table 1), while our current results for G3/99 test set give $a = 0.6$ (cf. Table 2). Also the BPW91h$_{abc}$, TPSSh, and revTPSSh$_a$ functionals perform differently on the two test sets.

4.4. Basis Set Effects. Our results show that simplification of the 6-311++G(3df, 3pd) to the 6-311+G(3df, 3pd) basis set leads to a slight overbinding that is proportional to the number of the H atoms in the molecule (cf. Table 2). The origin of this difference is simply the less negative H atom energy calculated with the + basis set compared to the diffuse ++ basis set. The molecular energies practically do not change. To demonstrate this, we have performed PBEh calculations with the 6-311++G(3df, 3pd) basis set and with a new basis set defined here (cf. Table 2). In the new 6-311+′G(3df, 3pd) basis set, the H atom is calculated with the 6-311++G(3df, 3pd) basis set, and all the molecules are calculated with the 6-311+G(3df, 3pd) basis set. The results agree very well as shown in Table 2. Comparison of the PBEh/6-311++G(3df, 3pd) and PBEh/6-311+G(3df, 3pd) results shows the slight relative overbinding of the latter smaller basis set (cf. ME = −1.51 and −1.74 kcal/mol and the −27.7 to −28.2 kcal/mol error for naphthalene in Table 2). Note that the difference is proportional to the number of H atoms. The smaller + basis set is considerably less expensive than the ++ basis set for H atom containing molecules, so for extensive comparisons the use of the smaller basis set is advantageous in computer time, without altering the conclusions.

Table 2. Summary of Deviations (ME, MAE) from Experiment of Standard Enthalpies of Formation, $\Delta_f H^o_{298}$, for the 223 Compounds of the G3/99 Test Set Computed with Various Methods Using Various Basis Sets[a]

functional	basis	*a*	*b*	*c*	ME	MAE	max	(+)	min	(-)	ref
BLYP	6-311++G(3df, 3pd)	0.00	1.00	1.00	3.81	9.49	41.0	(n-octane)	−28.1	(NO_2)	45
BPW91	6-311+G(3df, 3pd)	0.00	1.00	1.00	−5.58	9.03	21.4	($Si(CH_3)_4$)	−32.4	(NO_2)	this work
BPW91	6-311+G(2df, d)	0.00	1.00	1.00	−2.85	8.60	26.3	($Si(CH_3)_4$)	−31.0	(NO_2)	this work
PW86PBE	6-311+G(3df, 3pd)	0.00	1.00	1.00	−5.60	9.76	24.2	($Si(CH_3)_4$)	−36.1	(NO_2)	this work
PBE	6-311++G(3df, 3pd)	0.00	1.00	1.00	−21.69	22.22	8.7	(SiH_4)	−79.7	(azulene)	45
TPSS	6-311++G(3df, 3pd)	0.00	1.00	1.00	−5.20	5.81	16.2	(SiF_4)	−22.90	(ClF_3)	45
revTPSS	6-311+G(3df, 3pd)	0.00	1.00	1.00	−4.04	5.09	16.4	(SiF_4)	−25.70	(ClF_3)	this work
revTPSS	cc-pVTZ	**0.00**	**1.00**	**1.00**	−1.72	**4.54**	21.5	(SiF_4)	−22.90	(ClF_3)	this work
M06-2X[b]	6-311+G(3df, 3pd)	0.54	n.a.	n.a.	−1.33	**2.63**	15.6	(O_3)	−17.9	(P_4)	this work
B3LYP	6-311++G(3df, 3pd)	**0.20**	**0.72**	**0.81**	3.51	**4.93**	20.8	(SF_6)	−8.1	(BeH)	45
B3PW91	6-311++G(3df, 3pd)	**0.20**	**0.72**	**0.81**	−1.80	**3.90**	21.6	(SiF_4)	−17.0	(naphtalene)	45
BPW91h$_{abc}$	6-311+G(3df, 3pd)	**0.15**	**0.75**	**0.35**	1.57	**4.29**	26.9	(SF_6)	−9.3	(BeH)	this work
BPW91h$_{abc}$	6-311+G(3df, 3pd)	**0.15**	**0.79**	**0.75**	−0.70	**3.81**	22.4	(SiF_4)	−12.8	(pyrimidine)	this work
BPW91h$_a$	6-311+G(3df, 3pd)	0.15	0.85	1.00	2.59	5.37	24.7	(SiF_4)	−12.5	($F_2C{=}CF_2$)	this work
PW86PBEh$_a$	6-311+G(3df, 3pd)	0.15	0.85	1.00	2.50	6.19	27.8	(SiF_4)	−16.9	($C_4H_4N_2$)	this work
BPW91h$_{abc}$	6-311+G(3df, 3pd)	**0.20**	**0.70**	**0.57**	−0.04	**3.11**	23.7	(SiF_4)	−8.4	(BeH)	this work
BPW91h$_{abc}$	6-311+G(3df, 3pd)	**0.21**	**0.70**	**0.57**	1.84	**3.32**	25.3	(SiF_4)	−8.4	(BeH)	this work
PBE0	6-311++G(3df, 3pd)	0.25	0.75	1.00	−4.73	6.66	21.3	(SiF_4)	−35.6	(naphtalene)	45
PBEh$_a$	6-311++G(3df, 3pd)	**0.30**	**0.70**	**1.00**	−1.51	**4.89**	24.3	(SiF_4)	−27.7	(naphtalene)	this work
PBEh$_a$	6-311+'G(3df, 3pd)	**0.30**	**0.70**	**1.00**	−1.49	**4.89**	24.3	(SiF_4)	−27.7	(naphtalene)	this work
PBEh$_a$	6-311+G(3df, 3pd)	0.30	0.70	1.00	−1.74	5.02	24.3	(SiF_4)	−28.2	(naphtalene)	this work
PBEh$_a$	6-311+G(2df, d)	**0.30**	**0.70**	**1.00**	0.84	**4.91**	29.8	(SiF_4)	−24.7	(naphtalene)	this work
PBEh$_a$	6-311++G(3df, 3pd)	**0.32**	**0.68**	**1.00**	−0.23	**4.73**	25.5	(SiF_4)	−24.6	(naphtalene)	this work
PBEsolh$_a$	6-311+G(3df, 3pd)	0.20	0.80	1.00	−38.98	39.07	3.9	(Li_2)	−128.2	(naphtalene)	this work
PBEsolh$_a$	6-311+G(3df, 3pd)	0.25	0.75	1.00	−34.07	34.21	4.1	(Li_2)	−115.3	(naphtalene)	this work
PBEsolh$_a$	6-311+G(3df, 3pd)	0.50	0.50	1.00	−10.39	15.06	37.5	(O_3)	−56.2	(n-octane)	this work
PBEsolh$_a$	6-311+G(3df, 3pd)	0.60	0.40	1.00	−1.30	11.98	56.3	(O_3)	−41.1	(n-octane)	this work
TPSSh	6-311+G(3df, 3pd)	0.10	0.90	1.00	−0.86	**3.90**	22.0	(SiF_4)	−18.00	(Si_2H_6)	45
revTPSSh$_a$	6-311+G(3df, 3pd)	**0.10**	**0.90**	**1.00**	−0.06	**4.32**	22.2	(SiF_4)	−25.00	(ClF_3)	this work
revTPSSh$_a$	6-311++G(3df, 3pd)	0.20	0.80	1.00	3.91	6.60	27.7	(SiF_4)	−24.80	(Si_2H_6)	this work

[a] The geometries and zero-point energies were obtained at the B3LYP/6-31G(2df, p) level using a frequency scale factor of 0.9854. See also the footnote of Table 1. All values are in kcal/mol. Error = theory − experiment. 6-311+'G(3df, 3pd) basis set: all calculations were performed with 6-311+G(3df, 3pd), but the free H atom energy was calculated with the 6-311++G(3df, 3pd) basis set. [b] It was not possible to obtain self-consistent energy for Li atom. We calculated the energy using the PBE electron density. Less serious SCF convergence problems were observed for Na and several other atoms.

Further simplification of the 6-311+G(3df,3pd) basis sets by removing polarization functions leaves the atomic energies practically unchanged (especially for spherical atoms such as Li, Be, and N) but makes the molecular energies less negative and leads to an underbinding effect. Comparison of the BPW91/6-311+G(3df, 3pd) and BPW91/6-311+G(2df, p) results in Table 2 clearly shows this tendency. The general overbinding of BPW91 is partly compensated by the underbinding effect of the 6-311+G(2df, p) basis set compared to the 6-311+G(3df, 3pd) basis set (cf. ME = −5.6 vs −2.9 kcal/mol in Table 2). Even the MAE is slightly improved. Similar improvement can be observed for revTPSS/cc-pVTZ results in Table 2, in agreement with the observation that TPSS/6-311G(d, p) results[60] agree better with the experiment than the TPSS/6-311++G(3df, 3pd) results published in ref 45. Our results for the AE6 test set show that the PBE/cc-pVQZ and PBE/6-311+G(3df, 3pd) atomization energies are similar: The difference of the MAEs is less than 0.4 kcal/mol.

Table 3. Relative Percentage Errors, MPE, and MAPE of Calculated PBEsol and PBEsolh$_a$/6-311+G(3df, 3pd) Total Energies Compared to Best Estimates of Nonrelativistic Total Energies vs Weight of the Exact Exchange, *a*, of Eq 5 for Atoms and Molecules Included in AE6 Test Set[a]

		a (cf. eq 5)				
species	best energy hartree	0.00	0.25	0.40	0.50	0.60
H	−0.5000	−2.33	−1.38	−0.80	−0.42	−0.03
C	−37.8450	−0.59	−0.43	−0.34	−0.27	−0.21
O	−75.0674	−0.42	−0.31	−0.25	−0.20	−0.15
Si	−289.3600	−0.23	−0.17	−0.13	−0.11	−0.08
S	−398.1110	−0.20	−0.15	−0.12	−0.09	−0.07
SiH_4	−291.8738	−0.25	−0.18	−0.13	−0.11	−0.08
SiO	−364.7335	−0.27	−0.20	−0.16	−0.13	−0.11
S_2	−796.3840	−0.20	−0.15	−0.11	−0.09	−0.07
C_3H_4	−116.6582	−0.55	−0.41	−0.32	−0.26	−0.20
$C_2H_2O_2$	−227.8341	−0.44	−0.33	−0.27	−0.23	−0.18
C_4H_8	−157.2111	−0.55	−0.40	−0.31	−0.24	−0.18
MPE%		−0.55	−0.37	−0.27	−0.20	−0.12
MAPE%		0.55	0.37	0.27	0.20	0.12

[a] Nonrelativistic total energies are calculated from atomic energies in ref 80 and atomization energies in ref 70.

4.5. About the Origin of the Improvements. Table 3 shows the atoms and the molecules of the AE6 test set, the best estimates of the relevant total energies, the relative percentage errors (calculated/best estimate − 1) 100%, the mean percent errors (MPE%), and the mean absolute percent errors (MAPE%) of the calculated PBEsol/6-311+G(3df, 3pd) total energies as functions of the weight of the exact exchange, *a*, of eq 5. The best estimated energies for the molecules of the AE6 test are derived from the known atomic energies[80] and the reference atomization energies. The results in Table 3 show that the PBEsol functional ($a = 0.0$) gives

Table 4. Relative Percentage Errors, MPE, and MAPE of the Calculated 6-311+G(3df, 3pd) Total Energies Compared to Best Estimates of Nonrelativistic Total Energies vs Weight of Exact Exchange, *a*, of Eq 5 for Atoms and Molecules Included in AE6 Test Set[a]

		PBE	PBE0	PBEh$_a$	PW86PBE	BPW91	BPW91h$_a$	B3PW91	B3LYP
species	best energy hartree	$a = 0$	$a = 0.25$	$a = 0.32$	$a = 0$	$a = 0$	$a = 0.2$	$a = 0.2$	$a = 0.2$
H	−0.5000	−0.076	0.208	0.290	1.040	0.785	0.869	0.796	0.431
C	−37.8450	−0.135	−0.110	−0.103	0.076	−0.003	−0.001	−0.025	0.033
O	−75.0674	−0.084	−0.073	−0.069	0.073	0.014	0.010	−0.010	0.031
Si	−289.3600	−0.047	−0.038	−0.035	0.032	0.007	0.007	−0.007	0.012
S	−398.1110	−0.043	−0.034	−0.032	0.023	0.004	0.004	−0.008	0.006
SiH_4	−291.8590	−0.046	−0.035	−0.031	0.037	0.012	0.013	0.002	0.021
SiO	−364.7391	−0.054	−0.051	−0.049	0.039	0.007	0.001	−0.012	0.012
S_2	−796.4029	−0.043	−0.036	−0.033	0.022	0.004	0.003	−0.009	0.004
C_3H_4	−116.6851	−0.133	−0.122	−0.119	0.076	−0.007	−0.016	−0.031	0.014
$C_2H_2O_2$	−227.8833	−0.099	−0.102	−0.102	0.069	0.002	−0.014	−0.031	0.012
C_4H_8	−157.2426	−0.132	−0.112	−0.106	0.076	−0.004	−0.006	−0.020	0.017
MPE%		−0.081	−0.046	−0.035	0.142	0.075	0.079	0.059	0.054
MAPE%		0.081	0.084	0.088	0.142	0.077	0.086	0.087	0.054

[a] Nonrelativistic total energies are calculated from atomic energies in ref 80 and atomization energies in ref 70. Here B3PW91 and B3LYP are the original parametrizations of refs 32 and 56, respectively.

about −2.3% error for the H atom and −0.6% and −0.4% for the C and O atoms, respectively. It can be observed that relative percentage errors decrease with the increase of the atomic number (cf. −0.2% error for S atom). For molecules, the errors of the constituent atoms dominate in the error (cf. −0.2% error for S_2 molecule). Increasing the weight of the exact exchange consistently improves the performance of PBEsol for the total energies for the atoms and the molecules in the AE6 test set. The inclusion of exact exchange improves the PBEsol hybrid results for the right reason by improving the individual energies. We show the individual errors (calculated − best estimate) in the Supporting Information.

In Table 4 we present the same error analysis for the PBE, PBEh$_a$, PW86PBE, BPW91, BPW91h$_a$, B3PW91, and B3LYP functionals with the 6-311+G(3df, 3pd) basis set. The PBE energies are quite good and consistently more positive than the best-estimate energies (MPE% = −0.08%). Inclusion of exact exchange improves the MPE% via error compensation for PBEh$_a$. (The H atom energy is too negative by 0.9 kcal/mol or about 0.29% percent error, and all the other energies are too positive, cf. Supporting Information). But inclusion of exact exchange does not improve the MAPE%. The individual PBEh$_a$ errors do decrease compared to the PBE errors (cf. Supporting Information). A similar but larger (up to 3 kcal/mol, cf. Supporting Information) error occurs for the H atoms for all the other functionals shown in Table 4. Notice that PW86PBE, BPW91h$_a$, or B3PW91 give worse results than BPW91. B3LYP energies are all too negative, and B3LYP gives the smallest MPE% and MAPE%.

5. Ionization Potentials

Table 5 presents the ME and MAE for ionization potentials (IP) of the IP86[45] test set. IPs were calculated as the difference in total energies at 0 K of the cation and the corresponding neutral, at their corresponding B3LYP/6-31G(2df, p) geometries using scaled B3LYP/6-31G(2df, p) ZPEs. Calculations use the 6-311++G(3df, 3pd) and 6-311+G(2df, p) basis sets. The results show that these basis sets are practically equivalent for these calculations. Our results agree with the results in ref 45.

The best MAEs are slightly below 0.2 eV. The order of performance is B3LYP, PBEsolh, and BPW91h, with almost negligible differences between the functionals (set bold in Table 5). Generally a small underestimation (ME = −0.1, −0.2 eV) of IPs can be observed for nonhybrid functionals, and this underestimation is reduced by the inclusion of the exact exchange. PBEsol with $a = 0.6$ slightly overestimates the IPs (ME = 0.036 eV in Table 5). The ME shows again a quasilinear dependence on the value of *a* in eq 5. In general the hybrid functionals perform better than their nonhybrid counterparts, in agreement with ref 45.

The poorest ionization energy is predicted for the CN molecule because the open-shell $^1\Sigma^+$ singlet state of the CN^+ ion is not correctly described by the functionals used in this study.[66] The incorrect B3LYP geometries of the CH_4^+, BCl_3^+, $B_2F_4^+$, and BF_3^+ cations[81] also lead to large errors. (See the large deviations for BF_3^+ in Table 5.)

6. Electron Affinities

Anions are difficult test cases for the GGA, meta-GGA, and global hybrid functionals, as the self-interaction error can spoil the results. The results are also sensitive to the basis-set, which must be diffuse enough to describe anions but not more diffuse than that. We have calculated the electron affinity (EA) at 0 K as the difference between the total energies of the anion and the corresponding neutral species. We use the B3LYP/6-31G(2df, p) geometries.

Semilocal functionals lead to unstable negative atomic ions in the complete basis set limit, in which a fraction of an electron escapes. Nevertheless, realistic electron affinities can be computed using Gaussian basis sets in which the diffuse basis functions do not have characteristic decay lengths larger than those of the exact Kohn−Sham orbitals. In most cases, there is a plateau on which the electron affinity remains stable as the basis set is expanded within this range.[82]

Table 5. Summary of Deviations from Experiment of IPs of the G3/99 Test Set (86 species) Computed Using the 6-311++G(3df, 3pd) Basis Set[a]

method	basis	*a*	*b*	*c*	ME	MAE	max	(+)	max	(−)
BLYP	6-311++G(3df, 3pd)	0.00	1.00	1.00	−0.191	0.286	1.03	(CN)	−1.06	(BF_3)
BPW91	6-311++G(3df, 3pd)	0.00	1.00	1.00	−0.105	0.241	1.14	(CN)	−0.99	(BF_3)
BPW91	6-311+G(2df, p)	0.00	1.00	1.00	−0.105	0.238	1.15	(CN)	−0.96	(BF_3)
PBE	6-311+G(2df, p)	0.00	1.00	1.00	−0.105	0.233	1.12	(CN)	−0.98	(BF_3)
PBEsol	6-311+G(2df, p)	0.00	1.00	1.00	−0.146	0.237	1.06	(CN)	−0.96	(BF_3)
TPSS	6-311++G(3df, 3pd)	0.00	1.00	1.00	−0.134	0.242	1.22	(CN)	−1.02	(BF_3)
revTPSS	6-311++G(3df, 3pd)	0.00	1.00	1.00	−0.156	0.247	1.20	(CN)	−1.07	(BF_3)
B3LYP	6-311++G(3df, 3pd)	**0.20**	**0.72**	**0.81**	0.009	**0.184**	1.57	(CN)	−0.57	(B_2F_4)
B3PW91	6-311++G(3df, 3pd)	**0.20**	**0.72**	**0.81**	−0.012	**0.190**	1.58	(CN)	−0.65	(B_2F_4)
BPW91h$_a$	6-311+G(2df, p)	0.10	0.90	1.00	−0.084	0.218	1.35	(CN)	−0.77	(B_2F_4)
BPW91h$_a$	6-311+G(2df, p)	0.15	0.85	1.00	−0.074	0.210	1.45	(CN)	−0.72	(B_2F_4)
BPW91h$_a$	6-311+G(2df, p)	0.20	0.80	1.00	−0.064	0.204	1.55	(CN)	−0.67	(B_2F_4)
BPW91h$_{abc}$	6-311+G(2df, p)	**0.20**	**0.70**	**0.57**	0.079	**0.188**	1.67	(CN)	−0.51	(B_2F_4)
PBE0	6-311++G(3df, 3pd)	**0.25**	**0.75**	**1.00**	−0.064	**0.199**	1.61	(CN)	−0.67	(B_2F_4)
PBE0	6-311+G(2df, p)	**0.25**	**0.75**	**1.00**	−0.062	**0.198**	1.62	(CN)	−0.63	(B_2F_4)
PBEh$_a$	6-311+G(2df, p)	**0.32**	**0.68**	**1.00**	−0.051	**0.196**	1.76	(CN)	−0.57	(B_2F_4)
PBEsolh$_a$	6-311+G(2df, p)	**0.25**	**0.75**	**1.00**	−0.064	**0.186**	1.60	(CN)	−0.61	(B_2F_4)
PBEsolh$_a$	6-311+G(2df, p)	**0.60**	**0.40**	**1.00**	0.036	**0.198**	2.37	(CN)	−0.35	(Be)
TPSSh	6-311++G(3df, 3pd)	0.10	0.90	1.00	−0.113	0.229	1.41	(CN)	−0.79	(BF_3)
revTPSSh$_a$	6-311++G(3df, 3pd)	0.10	0.90	1.00	−0.129	0.230	1.40	(CN)	−0.80	(BF_3)
revTPSSh$_a$	6-311++G(3df, 3pd)	0.20	0.80	1.00	−0.102	0.219	1.59	(CN)	−0.62	(B_2F_4)

[a] The geometries and zero-point energies were obtained at the B3LYP/6-31G(2df, p) level using a frequency scale factor of 0.9854. All values are in eV. Error = calculated − experiment. The mean experimental IP is 10.89 eV. See also the footnote of Table 1. The best results (MAE < 0.2 eV) are in bold.

Table 6. Summary of Deviations from Experiment of EAs of the G3/99 Test Set[a]

method	basis	*a*	*b*	*c*	ME	MAE	max		min	
BLYP	6-311++G(3df, 3pd)	**0.00**	**1.00**	**1.00**	0.008	**0.115**	0.70	(C_2)	−0.26	(NCO)
BPW91	6-311++G(3df, 3pd)	**0.00**	**1.00**	**1.00**	0.035	**0.119**	0.78	(C_2)	−0.31	(NO_2)
BPW91	6-311+G(3df, 3pd)	**0.00**	**1.00**	**1.00**	0.030	**0.122**	0.78	(C_2)	−0.31	(NO_2)
BPW91	6-311+G(2df, p)	0.00	1.00	1.00	0.032	0.125	0.78	(C_2)	−0.29	(NO_2)
PBE	6-311+G(2df, p)	**0.00**	**1.00**	**1.00**	0.057	**0.121**	0.78	(C_2)	−0.28	(NO_2)
PBEsol	6-311++G(3df, 3pd)	**0.00**	**1.00**	**1.00**	0.039	**0.113**	0.74	(C_2)	−0.36	(NO_2)
TPSS	6-311++G(3df, 3pd)	0.00	1.00	1.00	−0.020	0.137	0.82	(C_2)	−0.32	(NO_2)
revTPSS	6-311++G(3df, 3pd)	0.00	1.00	1.00	−0.041	0.137	0.82	(C_2)	−0.33	(NO_2)
B3LYP	6-311++G(3df, 3pd)	**0.20**	**0.72**	**0.81**	0.088	**0.124**	1.10	(C_2)	−0.09	(HOO)
B3PW91	6-311++G(3df, 3pd)	0.20	0.72	0.81	0.031	0.137	1.08	(C_2)	−0.26	(HOO)
BPW91h$_a$	6-311+G(2df, p)	0.10	0.90	1.00	0.002	0.138	0.91	(C_2)	−0.28	(HOO)
BPW91h$_a$	6-311+G(2df, p)	0.15	0.85	1.00	−0.012	0.152	0.98	(C_2)	−0.3	(HOO)
BPW91h$_a$	6-311+G(2df, p)	0.20	0.80	1.00	−0.026	0.168	1.04	(C_2)	−0.33	(HOO)
BPW91h$_{abc}$	6-311+G(2df, p)	0.20	0.70	0.57	0.115	0.147	1.16	(C_2)	−0.13	(HOO)
PBE0	6-311+G(2df, p)	0.25	0.75	1.00	−0.028	0.172	1.10	(C_2)	−0.38	(HOO)
PBEh$_a$	6-311+G(2df, p)	0.32	0.68	1.00	−0.050	0.197	1.18	(C_2)	−0.42	(HOO)
PBEsolh$_a$	6-311+G(2df, p)	0.25	0.75	1.00	−0.016	0.150	1.10	(C_2)	−0.40	(HOO)
PBEsolh$_a$	6-311+G(2df, p)	0.60	0.40	1.00	−0.072	0.262	1.58	(C_2)	−0.61	(OH)
TPSSh	6-311++G(3df, 3pd)	0.10	0.90	1.00	−0.046	0.164	0.95	(C_2)	−0.33	(HOO)
revTPSSh$_a$	6-311++G(3df, 3pd)	0.10	0.90	1.00	−0.084	0.188	0.70	(C_2)	−0.41	(OH)
revTPSSh$_a$	6-311++G(3df, 3pd)	0.20	0.80	1.00	−0.061	0.170	0.95	(C_2)	−0.36	(HOO)

[a] The G3/99 has 58 species. Geometries and zero-point energies were obtained at the B3LYP/6-31G(2df, p) level using a frequency scale factor of 0.9854. All values are in eV. Error = theory − experiment. The mean experimental EA is 1.41 eV. See also the footnote of Table 1.

Table 6 presents the ME and MAE for electron affinities of the G3/99 test set (58 species, the EA58 test set is taken from ref 45). The open-shell singlet C_2 is isoelectronic with CN^+, and here again this electron structure causes a problem for single determinant GGAs, leading to extremely large errors in agreement with ref 45. The BPW91 results in the Table 6 show that the 6-311++G(3df, 3pd), 6-311+G(3df, 3pd), and 6-311+G(2df, p) basis sets are practically equivalent. The errors of the functionals are considerably larger than these basis set errors. Our study (not presented here) shows that omitting diffuse functions makes the errors very large.

The results in Table 6 show good agreement with the results in ref 45. GGAs slightly overbind the extra electron. The TPSS meta-GGA, however, shows a slight underbinding of the electron, and this is somewhat more pronounced for revTPSS. The BLYP and the PBEsol functionals show the best performance (MAE = 0.11 eV).

Table 7. Summary of Deviations from Experiment of PAs for the Eight Molecules of the G3/99 Test Set[a]

method	basis	*a*	*b*	*c*	ME	MAE	max	(+)	min	(−)
BLYP	6-311++G(3df, 3pd)	0.00	1.00	1.00	−1.46	1.57	0.4	(C_2H_2)	−3.9	(H_2O)
BPW91	6-311++G(3df, 3pd)	0.00	1.00	1.00	0.86	1.45	3.8	(C_2H_2)	−1.3	(PH_3)
BPW91	6-311+G(3df, 3pd)	0.00	1.00	1.00	0.86	1.47	3.8	(C_2H_2)	−1.3	(PH_3)
BPW91	6-311+G(2df, p)	0.00	1.00	1.00	0.68	1.27	3.4	(C_2H_2)	−1.4	(PH_3)
PBE	6-311++G(3df, 3pd)	0.00	1.00	1.00	−0.82	1.60	2.4	(C_2H_2)	−3.6	(PH_3)
PBEsol	6-311++G(3df, 3pd)	0.00	1.00	1.00	−2.69	2.88	0.7	(C_2H_2)	−6.8	(PH_3)
TPSS	6-311++G(3df, 3pd)	0.00	1.00	1.00	1.68	1.82	4.4	(C_2H_2)	−0.5	(H_2O)
revTPSS	6-311++G(3df, 3pd)	0.00	1.00	1.00	1.77	2.06	4.8	(C_2H_2)	−1.2	(H_2O)
B3LYP	6-311++G(3df, 3pd)	**0.20**	**0.72**	**0.81**	−0.77	**1.16**	1.6	(C_2H_2)	−2.3	(H_2)
B3PW91	6-311++G(3df, 3pd)	**0.20**	**0.72**	**0.81**	0.97	**1.07**	4.2	(C_2H_2)	−0.3	(SiH_4)
BPW91h$_a$	6-311+G(3df, 3pd)	0.10	0.90	1.00	1.08	1.32	4.3	(C_2H_2)	−0.5	(PH_3)
BPW91h$_a$	6-311+G(3df, 3pd)	0.15	0.85	1.00	1.20	1.26	4.5	(C_2H_2)	−0.1	(PH_3)
BPW91h$_a$	6-311+G(3df, 3pd)	0.20	0.80	1.00	1.31	1.33	4.7	(C_2H_2)	−0.1	(SiH_4)
BPW91h$_{abc}$	6-311+G(3df, 3pd)	0.20	0.70	0.57	1.22	1.27	4.1	(C_2H_2)	−0.1	(H_2O)
PBE0	6-311+G(3df, 3pd)	**0.25**	**0.75**	**1.00**	0.18	**1.14**	3.9	(C_2H_2)	−1.7	(SiH_4)
PBEh$_a$	6-311+G(3df, 3pd)	**0.32**	**0.68**	**1.00**	0.46	**1.10**	4.3	(C_2H_2)	−1.8	(SiH_4)
PBEsolh$_a$	6-311++G(3df, 3pd)	0.25	0.75	1.00	−1.25	1.88	2.5	(C_2H_2)	−4.2	(SiH_4)
PBEsolh$_a$	6-311++G(3df, 3pd)	0.50	0.50	1.00	0.22	1.66	4.4	(C_2H_2)	−3.7	(SiH_4)
PBEsolh$_a$	6-311++G(3df, 3pd)	0.60	0.40	1.00	0.82	2.04	5.1	(C_2H_2)	−3.5	(SiH_4)
TPSSh	6-311++G(3df, 3pd)	0.10	0.90	1.00	1.77	1.77	4.8	(C_2H_2)		
revTPSSh$_a$	6-311++G(3df, 3pd)	0.10	0.90	1.00	1.84	1.99	5.2	(C_2H_2)	−0.6	(H_2O)

[a] The geometries and zero-point energies were obtained at the B3LYP/6-31G(2df, p) level using a frequency scale factor of 0.9854. All values are in kcal/mol. Error = theory − experiment. The mean experimental PA is 158.0 kcal/mol. See also the footnote of Table 1.

Mixing exact exchange with the GGA or meta-GGA functionals shifts the ME to the electron-underbinding direction, and again we observed a quasilinear relationship between the value of a in eq 5 and the ME for BPW91h$_a$, PBEh$_a$, and PBEsolh$_a$. The example of BPW91h$_a$ shows that even $a = 0.1$ counterbalances the overbinding, but this does not improve the MAE value (cf. Table 6). This shows that for EA the inclusion of exact exchange deteriorates the results. The largest deterioration can be observed for functionals that underbind at the semilocal level (like TPSS or revTPSS) or for hybrids functionals with a large weight of exact exchange (cf. PBEsolh$_a$ in Table 6). This clearly shows a weakness of the global hybrids.

7. Proton Affinities

The proton affinity (PA) is calculated as the energy difference between the neutral and the protonated molecule M: PA(M) $= E_0(\mathrm{M}) - E_0(\mathrm{MH}^+)$. Adding a proton to a neutral molecule does not change the number of the electrons but alters the geometry and the distribution of the electron density. This usually leads to a more negative exchange and correlation energy.

We selected the eight PAs included in the G3/99 test set as published in ref 45 (the PA8 test set). We used the geometries and the scaled frequencies obtained at the B3LYP/6-31G(2df, p) level. Earlier results show that the LSDA seriously underbinds (ME = −5.9 kcal/mol), while the Hartree−Fock method slightly overbinds (ME = 1.8 kcal/mol), and these model chemistries give a poor MAE for the PA8 test set (MAE = 5.9 and 3.1 kcal/mol, respectively).

Table 6 presents the ME and MAE in proton affinities of the PA8 test set as in ref 45. Calculations use the 6-311++G(3df, 3pd), 6-311+G(3df, 3pd) and 6-311+G(2df, p) basis sets. The results show that the 6-311+G(2df, p) basis set error is large for the PA8 test set (cf. Table 7 BPW91 results), and thus we use only the 6-311+G(3df, 3pd) and 6-311++G(3df, 3pd) basis sets. The GGA functionals qualitatively differ from each other. The order of the GGA functionals from the most underbinding to the overbinding direction is PBEsol (closest to LSDA), BLYP, PBE, BPW91, TPSS, and revTPSS (ME = −2.7, −1.5, −0.8, +0.9, 1.7, and 1.8 kcal/mol, respectively, cf. Table 7). The hybrid functionals describe more correctly the protonation of PA8 and decrease the MAE from 1.5 to around 1 kcal/mol. The largest positive error was observed for C_2H_2 for all functionals.

As the BPW91 GGA overbinding is further aggravated by the overbinding effect of the exact exchange mixing, BPW91h$_a$ does not give good results (cf. Table 7). However, the reduced gradient contributions of exchange and correlation lead to some improvement [cf. MAE = 1.07 and 1.33 kcal/mol for B3PW91 and BPW91h$_{abc}$ ($a = 0.2$, $b = 0.8$, and $c = 1.0$) in Table 7]. This improvement is conserved in B3LYP results too (MAE = 1.16 kcal/mol). The underbinding of PBE is efficiently compensated by $a = 0.32$, and this hybrid is among the best functionals with MAE = 1.10 kcal/mol (cf. Table 7). The large proportion of exact exchange in PBEsolh$_a$ compensates the strong underbinding of PBEsol, but the MAE remains large (1.7−2.0 kcal/mol, Table 7). The TPSSh and revTPSSh$_a$ results conserve the overbinding errors of the parent functionals, that is slightly aggravated by the small portion of exact exchange ($a = 0.1$).

8. Bond Lengths and Visual Summary

Table 8 presents the ME and the MAE for equilibrium internuclear distances (r_e) of the T-96R test set as defined in ref 45. The geometry optimizations were carried out using the 6-311++G(3df, 3pd), 6-311G(2df, p), cc-pVTZ, and aug-cc-pVTZ basis sets with Opt = Tight and Int(Grid = Ultrafine) keywords. Comparison of the basis set dependence of the geometries shows that the 6-311G(2df, p) basis set gives similar, but slightly longer (by 0.010 Å), r_e values than the 6-311++G(3df, 3pd) basis set. This small deviation

Table 8. Summary of Deviations from Experiment of Equilibrium Bond Lengths (r_e) for the T96R Test Set[a]

method	basis	*a*	*b*	*c*	ME	MAE	max	(+)	max	(−)
BLYP	6-311++G(3df, 3pd)	0.00	1.00	1.00	0.0212	0.0223	0.055	(Al_2)	−0.032	(Na_2)
BPW91	6-311++G(3df, 3pd)	0.00	1.00	1.00	0.0166	0.0168	0.070	(Li_2)	−0.007	(F_2^+)
BPW91	6-311G(2df, p)	0.00	1.00	1.00	0.0178	0.0180	0.066	(Li_2)	−0.005	(F_2^+)
PBE	6-311G(2df, p)	0.00	1.00	1.00	0.0164	0.0170	0.052	(Li_2)	−0.008	(F_2^+)
PBEsol	6-311++G(3df,3pd)	0.00	1.00	1.00	0.0104	0.0127	0.067	(Li_2)	−0.021	(F_2^+)
TPSS	6-311++G(3df, 3pd)	0.00	1.00	1.00	0.0138	0.0142	0.078	(Li_2)	−0.008	(P_4)
TPSS	cc-pVTZ	0.00	1.00	1.00	0.0176	0.0180	0.062	(Li_2)	−0.013	(Be_2)
TPSS	aug-cc-pVTZ	0.00	1.00	1.00	0.0178	0.0182	0.062	(Li_2)	−0.014	(Be_2)
revTPSS	6-311++G(3df, 3pd)	0.00	1.00	1.00	0.0137	0.0141	0.081	(Li_2)	−0.010	(F_2^+)
B3LYP	6-311++G(3df, 3pd)	**0.20**	**0.72**	**0.81**	0.0050	**0.0104**	0.041	(Be_2)	−0.040	(Na_2)
B3PW91	6-311++G(3df, 3pd)	**0.20**	**0.72**	**0.81**	0.0026	**0.0093**	0.060	(Li_2)	−0.042	(F_2^+)
BPW91h$_a$	6-311G(2df, p)	0.10	0.90	1.00	0.0108	0.0127	0.064	(Li_2)	−0.024	(F_2^+)
BPW91h$_a$	6-311G(2df, p)	0.15	0.85	1.00	0.0076	0.0112	0.063	(Li_2)	−0.033	(F_2^+)
BPW91h$_a$	6-311G(2df, p)	0.20	0.80	1.00	0.0045	**0.0102**	0.065	(Be_2)	−0.041	(F_2^+)
BPW91h$_{abc}$	6-311G(2df, p)	**0.20**	**0.70**	**0.57**	0.0047	**0.0102**	0.059	(Be_2)	−0.038	(F_2^+)
PBE0	6-311G(2df, p)	**0.25**	**0.75**	**1.00**	0.0005	**0.0098**	0.069	(Be_2)	−0.050	(F_2^+)
PBEh$_a$	6-311G(2df, p)	0.32	0.68	1.00	−0.0033	0.0110	0.096	(Be_2)	−0.061	(F_2^+)
PBEsolh$_a$	6-311G(2df, p)	0.60	0.40	1.00	−0.0179	0.0249	0.231	(Be_2)	−0.098	(F_2^+)
TPSSh	6-311++G(3df, 3pd)	0.10	0.90	1.00	0.0068	**0.0096**	0.062	(Li_2)	−0.024	(F_2^+)
revTPSSh$_a$	6-311++G(3df, 3pd)	**0.10**	**0.90**	**1.00**	0.0070	**0.0100**	0.078	(Li_2)	−0.028	(F_2^+)
revTPSSh$_a$	6-311++G(3df, 3pd)	**0.20**	**0.80**	**1.00**	0.0020	**0.0091**	0.102	(Be_2)	−0.044	(F_2^+)

[a] All values are in Å. Error = calculated − experiment. The mean experimental r_e is 1.565 Å. See also the footnote of Table 1.

usually does not influence the total energies as the energy surfaces around the equilibria are flat. This is in agreement with the earlier observation that the 6-31G(2df, p) basis set gives reasonable geometries.[77] This is a useful observation to speed up considerably the calculations, as geometry optimizations with large diffuse basis sets are very slow and time consuming. The cc-pVTZ and aug-cc-pVTZ basis sets both give consistently longer (by 0.04 Å) r_e values than the 6-311++G(3df, 3pd) basis set as shown for TPSS (cf. Table 8). We have observed a similar 0.05 Å basis set effect for the average bond lengths calculated with the PBEsolh$_a$ functional (not shown in Table 8). This discrepancy shows that even large, polarized, and diffuse triple-ζ basis sets might introduce a considerable systematic error into the calculated equilibrium bond lengths.

It was observed for the T-96R test set that LSDA gives particularly good r_e values, and the Hartree−Fock method systematically underestimates the values of r_e (ME = −0.01 Å in Table 6 of ref 45, Be_2 excluded). We identified several problematic compounds in the T-96R: Be_2, Li_2, and Na_2. Be_2 has a large equilibrium distance and a very flat potential energy curve and is bound by a longer range dispersion interaction that is not described well by GGA or meta-GGA. Be_2 is unbound by the Hartree−Fock method. Although TPSS, PBE, and PBEsol bind Be_2,[83] inclusion of exact exchange makes r_e very large and leads to errors up to 0.231 Å (see PBEsolh (a = 0.6) in Table 8). We note that inclusion of the a posteriori dispersion correction at no cost considerably improves such results without deteriorating the covalent results.[84] Li_2 is problematic with all the functionals (too long r_e), but Na_2 is considerably better described with the hybrid functionals. The GGA and the hybrid results are spoiled by the self-interaction error for F_2^+. These results show that the weakly bound molecules are not described well with the functionals in this study.

While LSDA error compensation gives a reasonable prediction for the r_e values of the T-96R test set, the introduction of gradient correction (GGA and meta-GGA) gives too long r_e values, and that is efficiently compensated by the exact exchange. Again a quasilinear dependence of the ME on the value of exact exchange mixing (a in eq 5) was observed for BPW91h$_a$, PBEh$_a$, and PBEsolh$_a$ functionals. Notice that the ME value for BPW91h$_{abc}$ depends mainly on the value of a and shows much less dependence on b and c parameters of eq 7 (cf. Table 8). The best functionals are revTPSSh$_a$, B3PW91, TPSSh, PBEh$_a$, BPW91h$_a$, and B3LYP. All these functionals show MAEs about 0.01 Å in Table 8.

Visual Summary over the Test Sets. The summary of the statistics is visualized in Figure 4. The radar chart of the relative MAEs (kcal/mol) compared to B3LYP MAE for K9, G3/99, IP86, EA58, PA8, and T96R test sets shows, for example, that B3PW91 performs better or the same as B3LYP except for the EA58 test set, where hybrid functionals fail in general compared to the parent GGA. (Notice the better performance of BPW91 on the figure.)

9. Conclusions

Our formal discussion in Sections 1and 2 presented an explanation and a critique of the concept of global hybrid functionals.

Our numerical studies have introduced global hybrids starting from the previously unhybridized semilocal functionals PBEsol and revTPSS. Interestingly, PSEsol requires a large fraction (60%) of exact exchange to correct its strong overestimation of molecular atomization energies, and its hybrid then predicts accurate energy barriers and improved but still inaccurate atomization energies. But revTPSS requires only a small fraction (10%) of exact exchange to correct its slight overestimation of atomization energies, so its hybridization only slightly improves its strong underestimation of barriers.

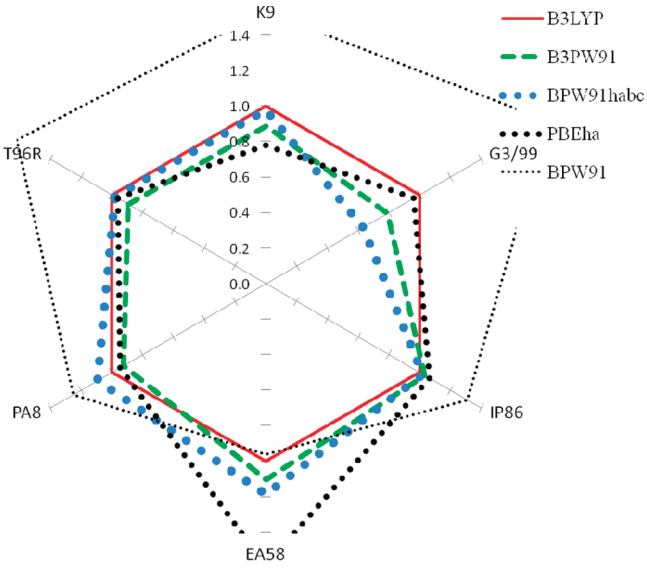

Figure 4. Radar or polar chart summary of the relative MAEs compared to B3LYP MAE (MAE(functional)/MAE(B3LYP)) for the K9, G3/99, IP86, EA58, PA8, and T96R test sets. The connecting lines are simply for guiding the eye. Smaller value means better performance.

We have also constructed optimized empirical parameters which surpass the standard ones for many popular hybrids, except the M06-2X hybrid meta-GGA that contains more than 30 empirical parameters. Perhaps the best overall performance is achieved by our refitted BPW91h$_{abc}$ (e.g., $a = 0.20$, $b = 0.70$, and $c = 0.57$, although different parameter combinations can produce similar results). Its performance seems better than that of the standard B3PW91, B3LYP, and PBE0. Our PBEh$_a$ with $a = 0.32$ also seems to perform better than the standard PBE0 with $a = 0.25$ for thermochemistry.

The molecular properties we have considered are those of the following test sets: G2-32 (32 ZPE-corrected atomization energies), AE6 (6 atomization energies), G3/99 (223 enthalpies of formation), BH6 (6 energy barriers), and K9 (kinetics) for thermochemistry as well as IP86 (86 ionizations), EA58 (58 electron affinities), PA8 (8 proton affinities), and T-96R (96 bond lengths). We tested B3LYP, B3PW91, BPW91, PBE, PW86PBE, PBEsol, TPSS, and revTPSS functionals and their global hybrids, using large triple-ζ basis sets. We also investigated the effects of fitting and basis sets. Here we will summarize the conclusions from our numerical studies in greater detail:

9.1. Test Sets. Our results show that the G2-32 test set is not suitable for testing the performance of any method for thermochemistry; the test set is not representative. The AE6 test set performs considerably better, but we obtained somewhat different results on the large G3/99 test set. The AE6 and the G3/99 test sets give different optimal weight of the exact exchange for the PBEsol functional. Moreover the BPW91h$_{abc}$, TPSSh, and revTPSSh$_a$ functionals perform differently on the two test sets.

The atomization energies for the molecules of the AE6 test set depend almost linearly on the weight of exact exchange, but this dependence varies. For five out of six molecules, the binding is reduced as the weight of exact exchange increases from zero, but SiH_4 shows the opposite behavior. Consequently the optimal weight of the exact exchange depends on the composition of the test set. Larger test sets are needed for reliable parameter optimizations.

9.2. Why B3LYP Works. The overbinding of the BPW91, PW86PBE, PBE, TPSS, revTPSS, and PBEsol functionals is efficiently compensated by a variable amount of exact exchange (with a larger overbinding requiring a larger portion of exact exchange). In contrast the BLYP functional typically underbinds. Since inclusion of exact exchange worsens the underbinding, it leads to worse results for BLYPh$_a$ on the AE6 and G3/99 test sets. The origin of the good results for B3LYP is the reduced gradient correction for the B88 exchange and the mixing of SVWN3 and LYP correlation. (In the first paragraph of Section 4, we corrected a numerical error in the literature that had overly favored B1LYP over B1PW91 on the nonrepresentative G2-32 test set.)

9.3. PBEsol Total Energies Are Improved Consistently by Hybridization. We observed for PBEsolh$_a$ on the AE6 test set that all atomic and molecular energies improve as the weight of the exact exchange increases to 60%. The total energies of other semilocal functionals can be overcorrected by hybridization. For example, PBEh$_a$ and other hybrid functionals give too negative H atom energies, and B3LYP gives too negative atomic and molecular energies for all components of the AE6 test set.

9.4. Hybrid Parameters *a*, *b*, and *c* Are Not Independent. In the three-parameter hybrids, the b and c parameters compensate each other's effects on the ME and partly on MAE. This shows that many different parametrizations might give practically the same results, as was demonstrated for several BPW91h$_{abc}$ hybrids.

9.5. Performance of Refitted Hybrid Functionals for Thermochemistry. We have constructed new BPW91h$_{abc}$, PBEh$_a$, PBEsolh$_a$, and revTPSSh$_a$ functionals. The best performer for the G3/99 test set is the BPW91h$_{abc}$ hybrid with $a = 0.20$, $b = 0.70$, and $c = 0.57$ (MAE = 3.1 compared to the MAE = 4.9 and 3.9 kcal/mol for the B3LYP and B3PW91 functionals). This functional performs particularly well for the AE6 test set (MAE = 2.1 compared to the MAE = 2.6 and 4.0 kcal/mol for the B3LYP and B3PW91 functionals). The new PBEh ($a = 0.32$) also performs better for the G3/99 test set than the original PBE0 ($a = 0.25$) (MAE = 4.7 vs 6.7 kcal/mol, respectively), and it performs better for the AE6 test set and for reaction kinetics (RMSE = 3.5 kcal/mol for the K9 test set). The PBEsolh$_a$ ($a = 0.60$) gives particularly accurate results for reaction kinetics (RMSE = 1.8 kcal/mol for the K9 test set), but it does not perform well for the G3/99 test set (MAE = 12.0 kcal/mol). The revTPSSh$_a$ ($a = 0.10$) shows good performance for the G3/99 test set (MAE = 4.3 kcal/mol), a small improvement over the revTPSS results (MAE = 5.0 kcal/mol). TPSSh performs slightly better (MAE = 3.9 kcal/mol) than revTPSSh$_a$.

9.6. Basis Sets. Simplification of the 6-311++G(3df, 3pd) to 6-311+G(3df, 3pd) basis sets leads to a slight overbinding that is proportional to the number of the H atoms in the molecule. The use of the smaller basis set is advantageous in computer time, without altering the conclusions. Further

simplification of the 6-311+G(3df, 3pd) basis set by removing polarization functions leads to underbinding. A general overbinding of a functional can be partly compensated by the underbinding effect of the 6-311+G(2df, p), 6-311G(d, p), or cc-pVTZ basis-sets. Comparison of the cc-pVQZ and 6-311+G(3df, 3pd) basis sets shows that these basis sets are close to the basis set limit for density functional theory (DFT) calculations.

9.8. Performance for Ionization Energies and Electron and Proton Affinities. For ionization potentials of the IP86 test set, the best MAEs are slightly below 0.2 eV. The order of performance is B3LYP, PBEsolh$_a$, and BPW91h$_a$, with negligible differences between the functionals. The ME shows again a quasilinear dependence on the value of a in eq 5. In general the hybrid functionals perform better than their nonhybrid counterparts, in agreement with ref 45. For several elements of the test set, the errors are large, as the open-shell $^1\Sigma^+$ singlet state of the CN^+ ion is not correctly described by the functionals and the B3LYP geometries of the CH_4^+, BCl_3^+,$B_2F_4^+$ and BF_3^+ cations used for calculations are incorrect.

For electron affinities (EA58 test set), the GGAs slightly overbind the extra electron. The TPSS meta-GGA however shows a slight underbinding of the electron, and this is somewhat more pronounced for revTPSS. The BLYP and the PBEsol functionals show the best performance (MAE = 0.11 eV). Mixing exact exchange with GGA or meta-GGA functionals shifts the ME to the electron-underbinding direction, and again we observed a quasilinear relationship between the value of a in eq 5 and the ME for BPW91h$_a$, PBEh$_a$, and PBEsolh$_a$. For EA58, inclusion of exact exchange deteriorates the results. The largest deterioration can be observed for functionals that underbind at the semilocal level (like TPSS or revTPSS) or for hybrids functionals with large weight of exact exchange (PBEsolh$_a$).

For proton affinities (PA8 set), the GGA functionals qualitatively differ from each other, and the order of the functionals from the most underbinding to the most overbinding is PBEsol, BLYP, PBE, BPW91, TPSS, and revTPSS (ME = −2.7, −1.5, −0.8, +0.9, 1.7, and 1.8 kcal/mol). The hybrid functionals describe more correctly the protonation and decrease the MAE from 1.5 to around 1 kcal/mol. The largest positive error was observed for C_2H_2 for all functionals.

9.7. Performance for Bond Lengths. While the LSDA error compensation gives a reasonable prediction for the r_e values of the T-96R test set, the introduction of gradient correction (GGA and meta-GGA) gives too long r_e values and is efficiently compensated by the exact exchange. Again a quasilinear dependence of the ME on the value of exact exchange mixing (a in eq 5) was observed for the BPW91h$_a$, PBEh$_a$, and PBEsolh$_a$ functionals. Notice that the ME values for BPW91h$_{abc}$ depend only on the value of a and show much less dependence on the b and c parameters of eq 7 (cf. Table 8). The best functionals are revTPSSh$_a$, B3PW91, TPSSh, PBEh, BPW91h$_a$, and B3LYP. All these functionals show MAEs about 0.01 Å. We identified several problematic compounds in the T-96R molecular geometry test set: Be_2, Li_2, and Na_2. Be_2 is bound by dispersion interaction that is not described well by GGA or meta-GGA. (It is unbound in the Hartree−Fock description.) Although TPSS, PBE, and PBEsol bind Be_2, inclusion of exact exchange makes r_e very large (with an error up to 0.231 Å). The dispersion-bound complexes cannot be described correctly by GGA, metaGGA, or global hybrid functionals. An a posteriori dispersion correction might remedy such errors at no cost by adding the missing C_6, C_8, and C_{10} terms.

Acknowledgment. This work was supported in part by the U.S. National Science Foundation under grant no. DMR-0854769. Computational resources were provided by the Center for Computational Science at Tulane University. This work is connected to the scientific program of the "Development of quality-oriented and harmonized R+D+I strategy and functional model at BME" project, supported by the New Hungary Development Plan (Project ID: TÁMOP-4.2.1/B-09/1/KMR-2010-0002).

Supporting Information Available: Zero-point energy corrected calculated atomization energies and statistical data for the molecules included in the G2-32 test set. Errors for the atoms and molecules included in the AE6 test set. This material is provided free of charge via the Internet at http://pubs.acs.org.

References

(1) Kohn, W.; Sham, L. J. *Phys. Rev. A* **1965**, *140*, 1133.

(2) Kurth, S.; Perdew, J. P. *Int. J. Quantum Chem.* **2000**, *77*, 814.

(3) Langreth, D. C.; Perdew, J. P. *Solid State Commun.* **1976**, *18*, 85.

(4) Gunnarsson, O.; Lundqvist, B. I. *Phys. Rev. B: Solid State* **1976**, *13*, 4274.

(5) Langreth, D. C.; Perdew, J. P. *Phys. Rev. B: Solid State* **1977**, *15*, 2884.

(6) von Barth, U.; Hedin, L. *J. Phys. C: Solid State Phys.* **1972**, *5*, 1629.

(7) Perdew, J. P.; Wang, Y. *Phys. Rev. B: Condens. Matter Mater. Phys.* **1992**, *45*, 13244.

(8) Langreth, D. C.; Mehl, M. *Phys. Rev. B: Condens. Matter Mater. Phys.* **1983**, *28*, 1809.

(9) Perdew, J. P.; Wang, Y. *Phys. Rev. B: Condens. Matter Mater. Phys.* **1986**, *33*, 8800. Perdew, J. P.; Wang, Y. *Phys. Rev. B: Condens. Matter Mater. Phys.* **1986**, *40*, 3399 (E).

(10) Perdew, J. P.; Chevary, S. H.; Vosko, S. H.; Pederson, M. R.; Singh, D. J.; Fiolhais, C. *Phys. Rev. B: Condens. Matter Mater. Phys.* **1992**, *46*, 6671. Perdew, J. P.; Chevary, S. H.; Vosko, S. H.; Pederson, M. R.; Singh, D. J.; Fiolhais, C. *Phys. Rev. B: Condens. Matter Mater. Phys.* **1993**, *48*, 4978 (E).

(11) Perdew, J. P.; Burke, K.; Ernzerhof, M. *Phys. Rev. Lett.* **1996**, *77*, 3865. Perdew, J. P.; Burke, K.; Ernzerhof, M. *Phys. Rev. Lett.* **1997**, *78*, 1396 (E).

(12) Perdew, J. P.; Burke, K.; Wang, Y. *Phys. Rev. B: Condens. Matter Mater. Phys.* **1996**, *54*, 16533. Perdew, J. P.; Burke, K.; Wang, Y. *Phys. Rev. B: Condens. Matter Mater. Phys.* **1998**, *57*, 14999 (E).

(13) Tao, J.; Perdew, J. P.; Staroverov, V.; Scuseria, G. E. *Phys. Rev. Lett.* **2003**, *91*, 146401.

(14) Perdew, J. P.; Ruzsinszky, A.; Csonka, G. I.; Vydrov, O. A.; Scuseria, G. E.; Constantin, L.; Zhou, X.; Burke, K. *Phys.*

Rev. Lett. **2008**, *100*, 136406. Perdew, J. P.; Ruzsinszky, A.; Csonka, G. I.; Vydrov, O. A.; Scuseria, G. E.; Constantin, L.; Zhou, X.; Burke, K. *Phys. Rev. Lett.* **2009**, *102*, 039902 (E).

(15) Perdew, J. P.; Ruzsinszky, A.; Csonka, G. I.; Constantin, L. A.; Sun, J. *Phys. Rev. Lett.* **2009**, *103*, 026403.

(16) Ernzerhof, M.; Perdew, J. P. *J. Chem. Phys.* **1998**, *109*, 3313.

(17) Constantin, L. A.; Perdew, J. P.; Tao, J. *Phys. Rev. B: Condens. Matter Mater. Phys.* **2006**, *73*, 205104.

(18) Constantin, L. A.; Perdew, J. P.; Pitarke, J. M. *Phys. Rev. B: Condens. Matter Mater. Phys.* **2009**, *79*, 075126.

(19) Becke, A. D. *Phys. Rev. A: At., Mol., Opt. Phys.* **1988**, *38*, 3098.

(20) Lee, C.; Yang, W.; Parr, R. G. *Phys. Rev. B: Condens. Matter Mater. Phys.* **1988**, *37*, 785.

(21) Becke, A. D.; Roussel, M. R. *Phys. Rev. A: At., Mol., Opt. Phys.* **1989**, *39*, 3761.

(22) Becke, A. D. *J. Chem. Phys.* **2003**, *119*, 2972.

(23) Roman-Perez, G.; Soler, J. M. *Phys. Rev. Lett.* **2009**, *103*, 096102.

(24) Dion, M.; Rydberg, H.; Schroeder, E.; Lundqvist, B. I. *Phys. Rev. Lett.* **2004**, *92*, 246401.

(25) Perdew, J. P.; Staroverov, V. N.; Tao, J.; Scuseria, G. E. *Phys. Rev. A: At., Mol., Opt. Phys.* **2008**, *78*, 052513.

(26) Perdew, J. P.; Savin, A.; Burke, K. *Phys. Rev. A: At., Mol., Opt. Phys.* **1995**, *51*, 4531.

(27) Ruzsinszky, A.; Perdew, J. P.; Csonka, G. I. *J. Phys. Chem. A* **2005**, *109*, 11006.

(28) Ruzsinszky, A.; Perdew, J. P.; Csonka, G. I.; Vydrov, O. A.; Scuseria, G. E. *J. Chem. Phys.* **2006**, *125*, 194112.

(29) Ruzsinszky, A.; Perdew, J. P.; Csonka, G. I.; Vydrov, O. A.; Scuseria, G. E. *J. Chem. Phys.* **2007**, *126*, 104102.

(30) Cohen, A. J.; Mori-Sanchez, P.; Yang, W. *Science* **2008**, *321*, 5890.

(31) Handy, N. C.; Cohen, A. J. *Mol. Phys.* **2001**, *99*, 403.

(32) Becke, A. D. *J. Chem. Phys.* **1993**, *98*, 1372.

(33) Becke, A. D. *J. Chem. Phys.* **1993**, *98*, 5648.

(34) Perdew, J. P.; Ernzerhof, M.; Burke, K. *J. Chem. Phys.* **1996**, *105*, 9982.

(35) Vydrov, O. A.; Scuseria, G. E. *J. Chem. Phys.* **2006**, *125*, 234109.

(36) Heyd, J.; Scuseria, G. E.; Ernzerhof, M. *J. Chem. Phys.* **2003**, *118*, 8207. Heyd, J.; Scuseria, G. E.; Ernzerhof, M. *J. Chem. Phys.* **2006**, *124*, 219906 (E).

(37) Ernzerhof, M.; Scuseria, G. E. *J. Chem. Phys.* **1999**, *110*, 5029.

(38) Adamo, C.; Barone, V. *J. Chem. Phys.* **1999**, *110*, 6158.

(39) Becke, A. D. *J. Chem. Phys.* **1997**, *107*, 8554.

(40) Zhao, Y.; Truhlar, D. G. *Acc. Chem. Res.* **2008**, *41*, 157.

(41) Jimenez-Hoyos, C. A.; Janesko, B. G.; Scuseria, G. E.; Staroverov, V. N.; Perdew, J. P. *J. Chem. Phys.* **2009**, *107*, 1077.

(42) Haunschild, R.; Janesko, B. G.; Scuseria, G. E. *J. Chem. Phys.* **2009**, *131*, 154112.

(43) Burke, K.; Cruz, F. G.; Lam, K.-C. *J. Chem. Phys.* **1998**, *109*, 8161.

(44) Tao, J.; Perdew, J. P.; Staroverov, V. N.; Scuseria, G. E. *Phys. Rev. A: At., Mol., Opt. Phys.* **2008**, *77*, 012509.

(45) Staroverov, V. N.; Scuseria, G. E.; Tao, J.; Perdew, J. P. *J. Chem. Phys.* **2003**, *119*, 12129. Staroverov, V. N.; Scuseria, G. E.; Tao, J.; Perdew, J. P. *J. Chem. Phys.* **2004**, *121*, 11507 (E).

(46) Kudin, K. N.; Scuseria, G. E.; Martin, R. L. *Phys. Rev. Lett.* **2002**, *89*, 266402.

(47) Brothers, E. N.; Izmaylov, A. F.; Normand, J. O.; Barone, V.; Scuseria, G. E. *J. Chem. Phys.* **2008**, *129*, 011102.

(48) Batista, E. R.; Heyd, J.; Hennig, R. G.; Uberagua, B. P.; Martin, R. L.; Scuseria, G. E.; Umrigar, C. J.; Wilkins, J. W. *Phys. Rev. B: Condens. Matter Mater. Phys.* **2006**, *74*, 121102.

(49) Perdew, J. P.; Levy, M. *Phys. Rev. Lett.* **1983**, *51*, 1884.

(50) Gruening, M.; Marini, A.; Rubio, A. *J. Chem. Phys.* **2006**, *124*, 154108.

(51) Furche, F.; Perdew, J. P. *J. Chem. Phys.* **2006**, *124*, 044103.

(52) Stroppa, A.; Kresse, G. *New J. Phys.* **2008**, *10*, 063020.

(53) Perdew, J. P.; Parr, R. G.; Levy, M.; Balduz, J. M. *Phys. Rev. Lett.* **1982**, *49*, 1691.

(54) Perdew, J. P.; Ruzsinszky, A.; Csonka, G. I.; Scuseria, G. E.; Staroverov, V. N.; Tao, J. *Phys. Rev. A: At., Mol., Opt. Phys.* **2007**, *76*, 040501.

(55) Dutoi, A. D.; Head-Gordon, M. *Chem. Phys. Lett.* **2006**, *422*, 230.

(56) Stephens, P. J.; Devlin, F. J.; Chabalowski, C. F.; Frisch, M. J. *J. Phys. Chem.* **1994**, *98*, 11623.

(57) Vosko, S. H.; Wilk, L.; Nusair, M. *Can. J. Phys.* **1980**, *58*, 1200.

(58) Kurth, S.; Perdew, J. P.; Blaha, P. *Int. J. Quantum Chem.* **1999**, *75*, 889.

(59) Redfern, P. C.; Zapol, P.; Curtiss, L. A.; Raghavachari, K. *J. Phys. Chem. A* **2000**, *104*, 5850.

(60) Csonka, G. I.; Ruzsinszky, A.; Tao, J.; Perdew, J. P. *Int. J. Quantum Chem.* **2005**, *101*, 506.

(61) Check, C. E.; Gilbert, T. M. *J. Org. Chem.* **2005**, *70*, 9828.

(62) Grimme, S. *Angew. Chem., Int. Ed.* **2006**, *45*, 4460.

(63) Paier, J.; Marsman, M.; Kresse, G. *J. Chem. Phys.* **2007**, *127*, 024103.

(64) Wodrich, M. D.; Corminboeuf, C.; Schleyer, P. v. R. *Org. Lett.* **2006**, *8*, 3631.

(65) Adamo, C.; Barone, V. *Chem. Phys. Lett.* **1997**, *274*, 242.

(66) Curtiss, L. A.; Redfern, P. C.; Raghavachari, K.; Pople, J. A. *J. Chem. Phys.* **1998**, *109*, 42.

(67) Lynch, B. J.; Truhlar, D. G. *J. Phys. Chem. A* **2003**, *107*, 8996. Lynch, B. J.; Truhlar, D. G. *J. Phys. Chem. A* **2004**, *108*, 1460 (E).

(68) Zhao, Y.; Lynch, B. J.; Truhlar, D. G. *J. Phys. Chem. A* **2004**, *108*, 2715. Boese, A. D.; Martin, J. M. L. *J. Chem. Phys.* **2004**, *121*, 3405.

(69) Zhao, Y.; Truhlar, D. G. *J. Phys. Chem. A* **2005**, *109*, 5656.

(70) Lynch, B. J.; Truhlar, D. G. Minnesota Database Collection, 2006; http://t1.chem.umn.edu/misc/database_group/database_therm_bh/ae6bh6.pl. Accessed October 10, 2010.

(71) Curtiss, L. A.; Raghavachari, K.; Redfern, P. C.; Pople, J. A. *J. Chem. Phys.* **2000**, *112*, 7374.

(72) Frisch, M. J. Trucks, G. W.; Schlegel, H. B.; Scuseria, G. E.; Robb, M. A.; Cheeseman, J. R.; Montgomery, Jr.; J. A.; Vreven, T.; Kudin, K. N.; Burant, J. C.; Millam, J. M.; Iyengar, S. S.; Tomasi, J.; Barone, V.; Mennucci, B.; Cossi, M.; Scalmani, G.; Rega, N.; Petersson, G. A.; Nakatsuji, H.; Hada, M.; Ehara, M.; Toyota, K.; Fukuda, R.; Hasegawa, J.; Ishida, M.; Nakajima, T.; Honda, Y.; Kitao, O.; Nakai, H.; Klene, M.; Li, X.; Knox, J. E.; Hratchian, H. P.; Cross, J. B.; Bakken, V.; Adamo, C.; Jaramillo, J.; Gomperts, R.; Stratmann, R. E.; Yazyev, O.; Austin, A. J.; Cammi, R.; Pomelli, C.; Ochterski, J. W.; Ayala, P. Y.; Morokuma, K.; Voth, G. A.; Salvador, P.; Dannenberg, J. J.; Zakrzewski, V. G.; Dapprich, S.; Daniels, A. D.; Strain, M. C.; Farkas, O.; Malick, D. K.; Rabuck, A. D.; Raghavachari, K.; Foresman, J. B.; Ortiz, J. V.; Cui, Q.; Baboul, A. G.; Clifford, S.; Cioslowski, J.; Stefanov, B. B.; Liu, G.; Liashenko, A.; Piskorz, P.; Komaromi, I.; Martin, R. L.; Fox, D. J.; Keith, T.; Al-Laham, M. A.; Peng, C. Y.; Nanayakkara, A.; Challacombe, M.; Gill, P. M. W.; Johnson, B.; Chen, W.; Wong, M. W.; Gonzalez, C.; Pople, J. A. *Gaussian 03*, revision D.02; Gaussian, Inc.: Wallingford, CT, 2004.

(73) Csonka, G. I.; Nguyen, N. A.; Kolossváry, I. *J. Comput. Chem.* **1997**, *18*, 1534.

(74) Zhao, Y.; Schultz, N. E.; Truhlar, D. G. *J. Chem. Theory Comput.* **2006**, *2*, 364.

(75) Zhao, Y.; Truhlar, D. G. *Theor. Chem. Acc.* **2008**, *120*, 215.

(76) Frisch, M. J.; Trucks, G. W.; Schlegel, H. B.; Scuseria, M. A. Robb, J. R. Cheeseman, G. Scalmani, V. Barone, B. Mennucci, G. A. Petersson, H. Nakatsuji, M. Caricato, X. Li, H. P. Hratchian, A. F. Izmaylov, J. Bloino, G. Zheng, J. L. Sonnenberg, M. Hada, M. Ehara, K. Toyota, R. Fukuda, J. Hasegawa, M. Ishida, T. Nakajima, Y. Honda, O. Kitao, H. Nakai, T. Vreven, J. A. Montgomery, Jr., J. E. Peralta, F. Ogliaro, M. Bearpark, J. J. Heyd, E. Brothers, K. N. Kudin, V. N. Staroverov, R. Kobayashi, J. Normand, K. Raghavachari, A. Rendell, J. C. Burant, S. S. Iyengar, J. Tomasi, M. Cossi, N. Rega, J. M. Millam, M. Klene, J. E. Knox, J. B. Cross, V. Bakken, C. Adamo, J. Jaramillo, R. Gomperts, R. E. Stratmann, O. Yazyev, A. J. Austin, R. Cammi, C. Pomelli, J. W. Ochterski, R. L. Martin, K. Morokuma, V. G. Zakrzewski, G. A. Voth, P. Salvador, J. J. Dannenberg, S. Dapprich, A. D. Daniels, Ö. Farkas, J. B. Foresman, J. V. Ortiz, J. Cioslowski , Fox, D. J. *Gaussian 09*, revision A.2; Gaussian, Inc.: Wallingford, CT, 2009.

(77) Curtiss, L. A.; Redfern, P. C.; Raghavachari, K.; Pople, J. A. *J. Chem. Phys.* **2001**, *114*, 108.

(78) Kannemann, F. O.; Becke, A. D. *J. Chem. Theory Comput.* **2009**, *5*, 719.

(79) Ruzsinszky, A.; Csonka, G. I.; Scuseria, G. E. *J. Chem. Theory Comput.* **2009**, *5*, 902.

(80) Chakravorty, S. J.; Gwaltney, S. R.; Davidson, E. R.; Parpia, F. A.; Fischer, C. F. *Phys. Rev. A: At., Mol., Opt. Phys.* **1993**, *47*, 3649.

(81) Baboul, A. G.; Curtiss, L. A.; Redfern, P. C.; Raghavachari, K. *J. Chem. Phys.* **1999**, *110*, 7650.

(82) Lee, D.; Furche, F.; Burke, K. *J. Phys. Chem. Lett.* **2010**, *1*, 2124, and references therein.

(83) Ruzsinszky, A.; Csonka, G. I.; Perdew, J. P. *J. Phys. Chem. A.* **2005**, *109*, 11015.

(84) Steinmann, S. N.; Csonka, G. I.; Corminboeuf, C. *J. Chem. Theory Comput.* **2009**, *5*, 2950, and references cited therein.

CT100488V